



J R C T E C H N I C A L R E P O R T S

Report of laboratory and in-situ validation of micro-sensor for monitoring ambient air pollution

012: CairClipO3/NO2 of
CAIRPOL (F)

Laurent Spinnelle
Michel Gerboles
Manuel Aleixandre

2013

Report EUR 26373 EN

European Commission
Joint Research Centre
Institute for Environment and Sustainability

Contact information

Michel Gerboles

Address: Joint Research Centre, Via Enrico Fermi 2749, TP 442, 21027 Ispra (VA), Italy

E-mail: michel.gerboles@ec.europa.eu

Tel.: +39 0332 78 5652

Fax: +39 0332 78 9931

<http://xxxx.jrc.ec.europa.eu/>

<http://www.jrc.ec.europa.eu/>

This publication is a Reference Report by the Joint Research Centre of the European Commission.

Legal Notice

Neither the European Commission nor any person acting on behalf of the Commission is responsible for the use which might be made of this publication.

Europe Direct is a service to help you find answers to your questions about the European Union

Freephone number (*): 00 800 6 7 8 9 10 11

(*) Certain mobile telephone operators do not allow access to 00 800 numbers or these calls may be billed.

A great deal of additional information on the European Union is available on the Internet.

It can be accessed through the Europa server <http://europa.eu/>.

JRC86479

EUR 26373 EN

ISBN 978-92-79-34832-7 (pdf)

ISSN 1831-9424 (online)

doi: 10.2788/4277

Luxembourg: Publications Office of the European Union, 20xx

© European Union, 2013

Reproduction is authorised provided the source is acknowledged.

Printed in Italy



ENV01- MACPoll Metrology for Chemical Pollutants in Air

**Report of the laboratory and in-situ validation of
micro-sensors and evaluation of suitability of
model equations**

O12: CairClipO3/NO2 of CAIRPOL (F)

Deliverable number: MACPoll_WP4_D435_O12_CairClipO3_NO2_V3

Version: 3.0 (Implementation of corrections of the collaborator)

Date: Nov. 2013

*Task 4.3: Testing protocol, procedures and testing of performances of sensors
(JRC, MIKES, INRIM, REG-Researcher (CSIC))*



JRC
JRC building 44 TP442
via E. Fermi 21027 - Ispra (VA)
Italy

Manuel Aleixandre (REG) - CSIC
Instituto de Física Aplicada,
Serrano 144 - 28006 Madrid
Spain

Reviewed by:
Olivier Zaouak (Cairpol)
MACCPoll Collaborator



1. TASK 4.3: TESTING PROTOCOL, PROCEDURES AND TESTING OF PERFORMANCES OF SENSORS (JRC, MIKES, INRIM, REG-RESEARCHER (CSIC)).....	7
1.1 “LABORATORY AND IN-SITU VALIDATION OF MICRO-SENSORS” AND “REPORT OF THE LABORATORY AND IN-SITU VALIDATION OF MICRO-SENSORS (AND UNCERTAINTY ESTIMATION) AND EVALUATION OF SUITABILITY OF MODEL EQUATIONS”	8
1.2 TIME SCHEDULE AND ACTIVITIES	8
1.3 PROTOCOL OF EVALUATION.....	9
1.4 GAS SENSOR TESTED WITHIN MACPoll.....	10
2 SENSOR IDENTIFICATION.....	11
2.1 MANUFACTURER AND SUPPLIER:.....	11
2.2 SENSOR MODEL AND PART NUMBER:.....	11
2.3 DATA PROCESSING OF THE SENSOR.....	11
2.4 AUXILIARY SYSTEMS SUCH AS POWER SUPPLY, TEST BOARD AND DATA ACQUISITION SYSTEM.	11
2.5 PROTECTIVE BOX/SENSOR HOLDER USED WITH THE MATERIAL USED FOR ITS PREPARATION.....	12
3 SCOPE OF VALIDATION	12
4 LITERATURE REVIEW:.....	13
5 LABORATORY EXPERIMENTS.....	14
5.1 EXPOSURE CHAMBER FOR TEST IN LABORATORY	14
5.2 GAS MIXTURE GENERATION SYSTEM	16
5.3 REFERENCE METHODS OF MEASUREMENTS.....	16
5.3.1 <i>Methods</i>	16
5.3.2 <i>Quality control</i>	17
5.3.3 <i>Homogeneity</i>	17
6 METROLOGICAL PARAMETERS.....	17
6.1 RESPONSE TIME	17
6.2 PRE CALIBRATION.....	19
6.3 REPEATABILITY, SHORT-TERM AND LONG-TERM DRIFTS.....	21
6.3.1 <i>Repeatability</i>	21
6.3.2 <i>Short term drift</i>	22
6.3.3 <i>Long term drift</i>	23
7 INTERFERENCE TESTING	25
7.1 GASEOUS INTERFERING COMPOUNDS	25
7.1.1 <i>Nitrogen dioxide</i>	27
7.1.2 <i>Nitrogen monoxide</i>	28



7.1.3	Carbon monoxide interference.....	28
7.1.4	Carbon dioxide interference.....	29
7.1.5	Sulfur dioxide interference	29
7.1.6	Ammonia interference.....	29
7.2	AIR MATRIX.....	30
7.3	HYSTERESIS.....	32
7.4	METEOROLOGICAL PARAMETERS	33
7.4.1	Temperature and humidity.....	33
7.4.2	Wind velocity effect.....	36
7.5	EFFECT OF CHANGE OF AMBIENT PRESSURE	37
7.6	EFFECT OF CHANGE IN POWER SUPPLY	38
7.7	CHOICE OF TESTED INTERFERING PARAMETERS IN FULL FACTORIAL DESIGN.....	38
8	EXPERIMENTAL DESIGN.....	39
8.1	UNCERTAINTY ESTIMATION.....	43
9	FIELD EXPERIMENTS.....	44
9.1	MONITORING STATIONS.....	44
9.2	SENSOR EQUIPMENT.....	46
9.3	CHECK OF THE SENSOR IN LABORATORY	46
9.4	FIELD RESULTS	47
9.5	ESTIMATION OF FIELD UNCERTAINTY.....	51
9.6	CALIBRATION.....	52
10	CONCLUSIONS.....	55
11	APPENDIX A: TECHNICAL DATA SHEET CAIRCLIP O₃-NO₂.....	56
12	APPENDIX B: RESPONSE TIME STEPS.....	57

1. Task 4.3: Testing protocol, procedures and testing of performances of sensors (JRC, MIKES, INRIM, REG-Researcher (CSIC))

The aim of this task was to validate NO₂ and O₃ cheap sensors under laboratory and field conditions and when sensors are transported by human beings or vehicles in different micro-environments for the assessment of human exposure. Based on the recommendations of the review (Task 4.1), the graphene sensors and a limited number of sensor types and air pollutants were chosen. At the beginning of the validation a testing protocol was drafted, which was improved and refined during the process of validation experience. This task provided the information needed for estimating the measurement uncertainty of the tested sensors. Further, procedures for the calibration of sensors able to ensure full traceability of measurements of sensors to SI units were also drafted.

The laboratory work package endeavours to find a solution to the current problem of validation of sensors. In general, the validation of sensors is either carried out in a laboratory using synthetic mixtures, or at an ambient air monitoring station with real ambient matrix. Generally, these results are not reproducible at other sites than the one used during validation. In fact, sensors are highly sensitive to matrix effects, meteorological conditions and gaseous interferences that change from site to site.

Commonly, the validation generally performed by sensor users consists in establishing the minimum parameter set of sensors to describe their selectivity, sensitivity and stability. Since, this features is generally not reproducible from site to site, it was proposed in this project to extend the validation procedure by establishing simplified model descriptions of the phenomena involved in the sensor detection process. Both laboratory experiment in exposure chambers and fine tuning of these models during field experiments were carried out in this project.

The sensors were exposed to controlled atmospheres of gaseous mixtures in exposure chambers. These laboratory controlled atmospheres consisted of a set of mixtures with several levels of NO₂/O₃ concentrations, under different conditions of temperature and relative humidity and including the main gaseous interfering compound.

Description of work:

- The tested sensors were selected by CSIC and JRC. The development of the protocol for the evaluation of sensors was carried out by CSIC and JRC. INRIM and MIKES carried out the initial laboratory evaluations of the new NO₂ graphene sensors. JRC carried out the experimental test of the selected O₃ and NO₂ commercial sensors and JRC and the REG-Researcher (CSIC) performed the evaluation of their test results. After laboratory tests, the commercial O₃ and NO₂ sensors were tested at field sites under real conditions by JRC.
- Along the different step of the project, the protocol for evaluation of sensors was improved by CSIC and JRC based on the test results and the technical feasibility of the experiments.
- The controlled atmospheres of the INRIM and MIKES tests were designed to evaluate the linearity of graphene sensors at different NO₂ levels (5) and their stability with respect to temperature (3 levels) and/or relative humidity (3 levels) at constant NO₂ level.
- JRC performed laboratory tests to determine the parameters of the NO₂ and O₃ model equations (task 4.1) using full or partial experimental design of influencing variables (identified in task 4.1). In any case, the controlled atmosphere included at least 5 levels of air pollutants, 3 levels of air pollutants and 3 levels of relative humidity and 2 levels of the chemical interference evidenced in task 4.1.
- CSIC and JRC applied the protocol of evaluation to the commercial sensors with determination of their metrological characteristics: detection limits, response time, poisoning points, hysteresis, etc., measurement uncertainty in laboratory and field experiment.

Activity summary: (The text with yellow background shows the activity reported in this report)

1. Selection of suitable sensors for validation (at least 2 commercially available NO₂ sensors, 3 commercially available O₃ sensors and the INRIM and MIKES graphene sensors **(JRC, REG-Researcher (CSIC))**)
2. Development of a validation protocol and procedures for calibration of micro-sensors **(CSIC)**



3. Laboratory evaluation of the INRIM and MIKES graphene sensors: lab tests of NO₂ level, temperature, humidity, response time and hysteresis **(INRIM)**
4. Laboratory evaluation of the INRIM and MIKES graphene sensors (lab tests of NO₂ concentration, response time, warming time and temperature or humidity effect) **(MIKES)**
5. Laboratory tests in exposure chamber and at one field site according to the validation protocol **(JRC)**. The site will be representative of the population exposure and should be consistent with the sampling sites in which micro-sensors are likely to be used in future. Unless the bibliographic review will suggest other locations for any reason, the O₃ sensors will be tested at a suburban/rural site (at the JRC). The sampling site for NO₂ will be representative for urban areas or traffic sites where high levels of NO₂ in conjunction with sufficient population density are expected. Nevertheless, the actual location of the field site will be confirmed after the bibliographic review.
6. Improvement of graphene sensors based on the results of JRC laboratory tests **(INRIM, MIKES)**
7. Estimation of the effect of influencing variables based on laboratory and field tests and evaluation of the suitability of the model equations proposed in 4.1 **(REG-Researcher (CSIC), JRC)**

This task leads to deliverables 4.3.1 -4.3.5.

1.1 “Laboratory and in-situ validation of micro-sensors” and “Report of the laboratory and in-situ validation of micro-sensors (and uncertainty estimation) and evaluation of suitability of model equations”

1.2 Time schedule and activities

4.3.4	Laboratory and in-situ validation of micro-sensors	JRC	INRIM, MIKES	Data sets	Jul. 2013
4.3.5	Report of the laboratory and in-situ validation of micro-sensors (and uncertainty estimation) and evaluation of suitability of model equations	JRC	INRIM, MIKES, REG-Researcher (CSIC)	Report	Dec. 2013

1.3 Protocol of evaluation

This report presents the evaluation of the performances of the Cairclip sensor of Cairpol according to the MACPoll Validation protocol[1]. The objective of this evaluation was to determine the uncertainty of the sensor values obtained in the laboratory and field conditions and to further compare these uncertainty with the Data Quality Objective (DQO) of the European Air Quality Directive[2] for indicative method. The DQOs correspond to a relative expanded uncertainty of measurement. A flow chart depicting the procedure for the validation of sensors is given in Figure 1.

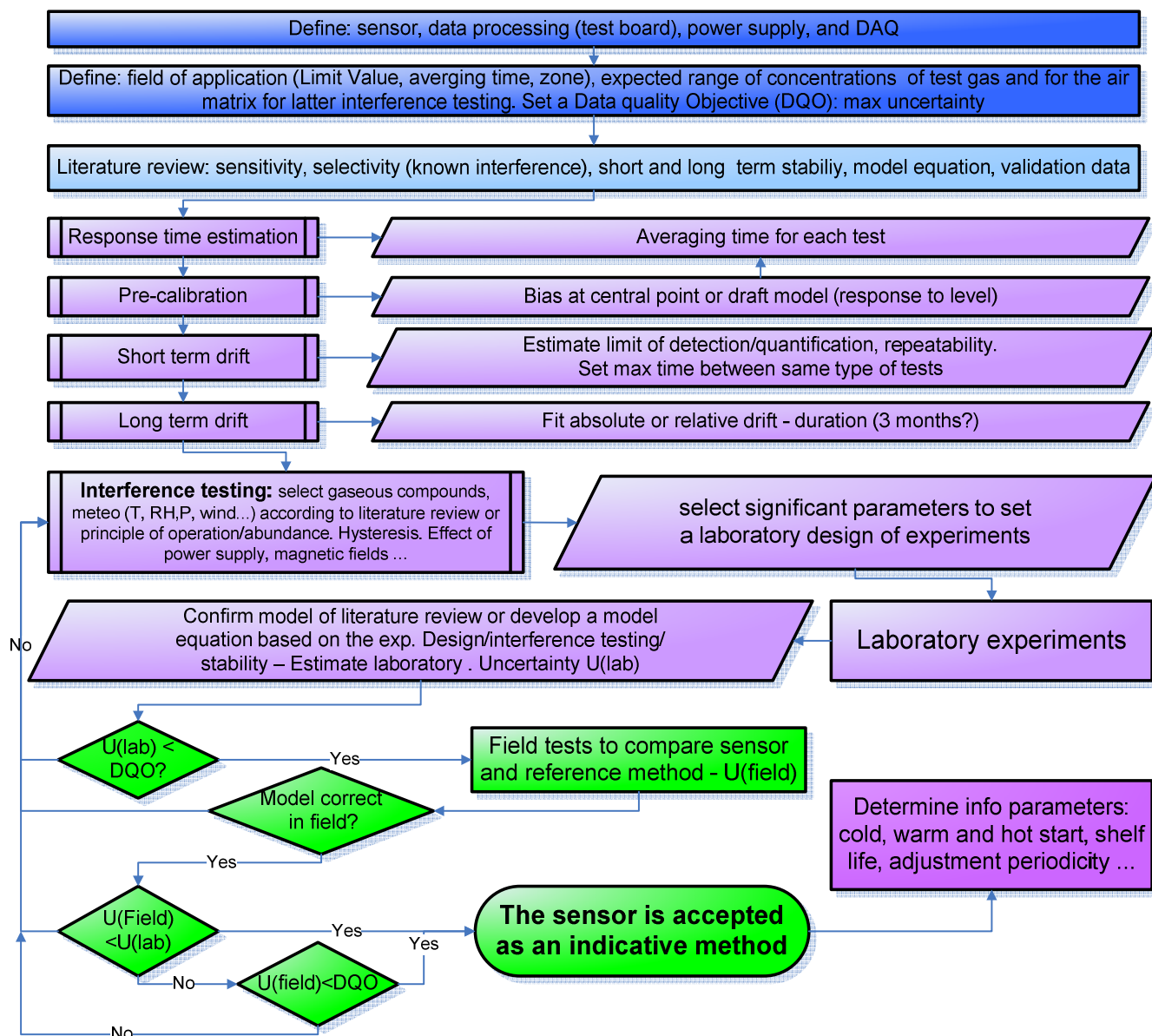


Figure 1: Protocol of evaluation of sensor

¹ Spinelle L, Alexandre M, Gerboles M. Protocol of evaluation and calibration of low-cost gas sensors for the monitoring of air pollution. EUR 26112. Luxembourg (Luxembourg): Publications Office of the European Union; 2013. JRC83791. Revision of the validation protocol and procedure for calibration, ENV01- MACPoll Metrology for Chemical Pollutants in Air, Deliverable number: (4.3.3), Vs 1.0, Jun 2013, Task 4.3: Testing protocol, procedures and testing of performances of sensors (JRC, MIKES, INRIM, REG-Researcher (CSIC))

² Directive 2008/50/EC of the European Parliament and the Council of 21 May 2008 on ambient air quality and cleaner air for Europe

Table 1: Matrix of laboratory tests carried out in exposure chamber under controlled conditions

	Tests	Temperature, °C	Relative humidity, %	Comment
1	Response Time	Mean	Mean	Three times: 0 to 80 % of Full Scale and 80% of FS to 0
2	Pre-calibration	Mean	Mean	At least 3 levels including 0, LV, IT, AT, CL, LAT and UAT
3	Repeatability, short-long term drifts			
3-1	Repeatability	Mean	Mean	0 and 80 % of LV, 3 repetitions every averaging time
3-2	Short term drift	Mean	Mean	0, 50 % and 80 % of LV, 3 repetitions per day for 3 consecutive days
3-3	Long term drift	Mean	Mean	0, 50 % and 80 % of LV, repeated every 2 weeks during 3 months
4	Interference testing			
4-1	Air matrix	Mean	Mean	Zero air, laboratory air and ambient air at pre-calibration levels
4-2	Gaseous interference	Mean	Mean	Interfering compound at 0 and mean level, test gas at LV and 0
4-3	Temperature	Mean-10 °C, mean and mean+10 °C	Mean	At LV
4-4	Humidity	Mean	Mean-20%, mean and mean+20%	At LV
4-5	Hysteresis	Mean	Mean	Increasing-decreasing-increasing concentration cycles of the pre-calibration levels
4-6	Pressure	Mean	Mean	Ambient pressure + 10 mbar and Ambient pressure - 10 mbar
4-7	Power supply effect	Mean	Mean	At LV, test under 210, 220 and 230 V
4-8	Wind velocity	Mean	Mean	Between 1 and 5 m/s (only if needed)
4	Validation/modelling			
4-1	Lab experiments (model)	Mean-10°C, mean, mean +10°C, if found significant	Mean-20%, mean, mean +20 %, if found significant	pre-calibration levels under: temperature and humidity (3 levels) and interference (2 levels)
4-2	Field experiments			At an automatic station equipped with reference method of measurements
5	Additional information			
5-1	Cold start, warm start, hot start	Mean	Mean	At LV

CL: Critical levels for the protection of the vegetation, , FS: Full Scale, IT/AT: Information and alert thresholds, LAT: Lower assessment threshold, LV: Limit values or target value, Mean: average temperature or humidity observed in the field of application, UA: Upper assessment threshold

Table 1 gives a list of all the tests for the evaluation of micro-sensors included in the protocol [1]. Even when the DQO would not be met the application of the protocol is still of interest as the method produces a full estimation of laboratory and field measurement uncertainty which demonstrates the performance of the sensor.

1.4 Gas sensor tested within MACPoll

Within MACPoll, Work Package 4, eleven models of ozone (O₃) sensors were selected for evaluation (see Table 2). Hereafter, we report the results of the evaluation of the ozone sensor of Cairpol (yellow background in Table 2) which is a chemical sensor.

Table 2: List of O₃ sensors selected for the MACPOL validation programme (this report gives the evaluation of the sensor with yellow background)

N°	Manufacturer	Model	Type	Data acquisition
O1	Unitec s.r.l	O ₃ Sens 3000	Res.	Analogic voltage of transmitter board
O2	Ingenieros Assessores	Nano EnviSystem mote and MicroSAD datalogger, with Oz-47 sensor	Res.	File transfer of data logger
O3	αSense	O ₃ sensors B4	4 Elect.	Analogic Voltage of transmitter board
O4	Citytech	Sensoric 4-20 mA Transmitter Board with O3E1 sensor	3 Elect.	Analogic Voltage of transmitter board
O5	Citytech	Sensoric 4-20 mA Transmitter Board with O3E1F sensor	3 Elect.	Analogic Voltage of transmitter board
O6	Citytech	A3OZ EnviroceL -	4 Elect.	No testing board existing?
O7	SGX Sensortech	MiCS-2610 sensor and OMC2 datalogger,	Res.	File transfer of data logger
O8	SGX Sensortech	MiCS Oz-47 sensor and OMC3 datalogger	Res.	File transfer of data logger
O9	SGX Sensortech	MiCS Oz-47 sensor with JRC test board	Res.	Development of a digital driver
O10	IMN2P	Prototype WO ₃ sensor with MICS-EK1 Sensor Evaluation Kit	Res.	File transfer of the data logger
O11	FIS	SP-61 sensor and evaluation test board	Res.	Analogic Voltage of transmitter board
O12	CairPol – F	CairclipO ₃ /NO ₂	3 Elect.	Analogic Voltage of transmitter board embedded in the sensor

3 Elect. and 4 Elect.: amperometric, 3 or 4 electrode sensor, Res.: resistive sensor

2 Sensor Identification

2.1 Manufacturer and supplier:

CAIRPOL, ZAC du Capra, 55, avenue Emile Antoine, 30340 Méjames les Alès – France, Tel: +33 (0)4 66 83 37 56, Fax: +33 (0)4 66 61 82 53, info@cairpol.com, www.cairpol.com

2.2 Sensor model and part number:

Sensors: Cairclip O₃/NO₂ ANA (analogic model), serial number (s/n) CCB0306120001 (used for the field experiments) and CCB0306120002 (used in the laboratory experiments). The sensors were not calibrated by the manufacturer.

Another Cairclip sensor, the CairClipNO₂ sensor was tested for the effect of O₃ on its response. This results are reported in the MACPoll report for the CairClipNO₂ sensor [3].

2.3 Data processing of the sensor

No info was available about any embedded data processing system that may change the sensor responses.

2.4 Auxiliary systems such as power supply, test board and data acquisition system.

A few options were included with the sensor. They consisted of: dongles USB (red for switching off the sensor, see Figure 2, and green used as a sensor base), filters, USB cable, and USB power supply.

- Power supply: a TracoPower-ESP18-05SN 5V-3.6-A power supply was used both for the laboratory tests and field tests. The power supply supplied by Cairpol was not used.
- Test board: no need for a test board, Cairclip sensors include a 5V output on their USB connector.
- Data acquisition: the data acquisition board was a National Instrument, 14 bits Analog-to-digital converter, NI-USB 6009 (National Instruments USA), NI USB 6009, USB powered. The periodicity of data acquisition was set to 100 Hz in order to eliminate electronic noise out of minute averages without further filtering needed. Within the DAQ, the sensor responses consisting in a voltage output in V were transformed into a mole ratio of O₃ using the equation given in the data sheet of the sensor: $O_{3,nmol/mol} = (1000 V - 100)/10$ where V is the sensor response in V.

³ Report of laboratory and in-situ validation of micro-sensor for monitoring ambient air pollution, NO₉: CairClipNO₂ of CAIRPOL (F), to be published

2.5 Protective box/sensor holder used with the material used for its preparation

During the laboratory test in the exposure chamber, the Cairclip sensors (see Figure 2) were used without any protection box. Figure 2, upper right, shows examples of sensors installed in the exposure chamber (these are other sensors – not the CairClip sensor). For the field tests, the sensors were included into a PVC box (see Figure 2) together with other 2 other sensors.



Figure 2: Upper left: view of the Cairclip sensor; upper right: example of an ozone sensor in the exposure chamber; bottom left: ClairClip sensors installed in a PVC box at the field monitoring site.

3 Scope of validation

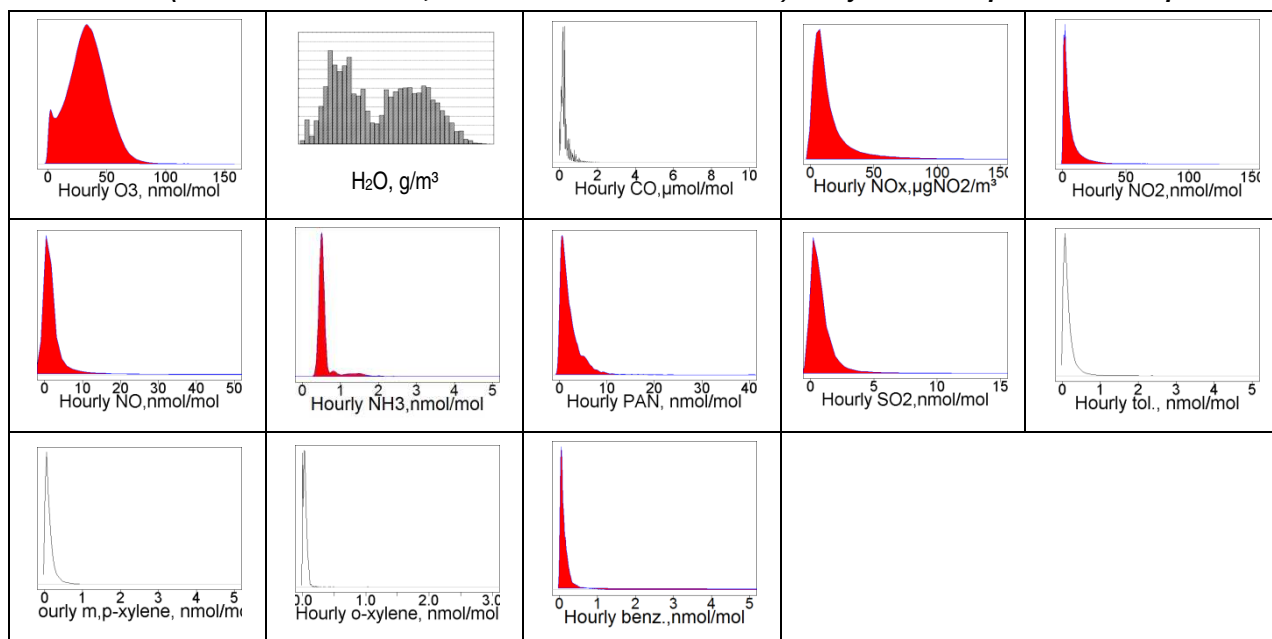
The aim of this study was to demonstrate whether or not the Cairclip sensor satisfies the Data Quality Objective (DQO) for O₃ Indicative Methods at the O₃ target level (LV). The following conditions apply:

- the DQO consists of a relative expanded uncertainty of 30 % in the region of the Target Value (LV)
- the LV corresponds to 120 µg/m³ or 60 nmol/mol
- the LV is defined as an 8-hour mean computed from hourly averages. Consequently, an averaging time of one hour is mandatory. Other important values defined in the Directive are the AOT40, 40 µg/m³ (20 nmol/mol), the information and alert thresholds (IT/AT): 180 µg/m³ (90 nmol/mol) and 240 µg/m³ (120 nmol/mol), respectively.
- it is planned to validate the sensor in the following micro-environment: at background stations in rural areas since they corresponds to zones where O₃ monitoring is mandatory.



Using several on-line databases and literature sources, Table 3 was established to set down the expected air composition in different micro-environments. More details are given in [4]. Using this table, the full scale of the ozone gas sensor was set to 120 nmol/mol with main mode at 60 nmol/mol. Major gas molecules in rural zones appears to be H₂O, CO, NO₂.

Table 3: Ambient air composition at background stations and rural areas between 2008 and 2010 relevant to O₃ and NO₂ (data from the Airbase, EUsar and TTorchs databases). Daily data are reported unless specified.



Further to this information it was decided to:

- set the full scale to the alert threshold: about 120 nmol/mol. In table 3, the maximum O₃ hourly mean is over 150 nmol/mol while the 95th percentile is about 75 nmol/mol
- to check the interference of abundant compounds: H₂O, CO, NO₂/NO, NH₃, and SO₂ to a lesser extent. PAN was not considered because it is too difficult to generate and control.
- the mean temperature and mean relative humidity were set to 22 °C and 60 %, respectively.

It is worth reminding that before using the sensor based on the validation data included in this report, it should be ascertained that the sensor is applied in the same configuration in which it was tested here. This requires using the same data acquisition and processing, the same protection box and calibration type. The sensor shall be submitted to the same regime of QA/QC as during evaluation. In addition, it is strongly recommended that sensors results are periodically compared side-by-side using the reference method.

4 Literature review:

Category under which the gas sensor falls:

- the sensor behaves as a black-box without the user knowing the model equation used for the transformation of sensor response into O₃ values,
- the company does not supply information about the relevant data treatment and processing that is applied and the model equation used for the transformation of the sensor responses into O₃ values
- the objective of this evaluation protocol was the validation of the sensor O₃ values with the possibility to establish a correction function with the test results of the evaluation protocol if needed.

No info was found on the internet about the performance of this sensor, except a short presentation [5]

⁴ MACPoll, WP4, Selection of suitable micro-sensors for validation, D4.3.1, vs 1, Mar 2012

⁵ <https://sites.google.com/site/airsensors2013/final-materials>, session Air Sensors Evaluation Project, EPA's Next Generation Air Monitoring Workshop Series, Air Sensors 2013: Data Quality & Applications, March 19 & 20, 2013, EPA's Research Triangle Park Campus, 109 T.W. Alexander Drive, Research Triangle Park, North Carolina 27711, Ron Williams, Russell Long, Melinda Beaver, (U.S. EPA), Keith Kronmiller, Sam Garvey, (Alion), Olivier Zaouak (Cairpol)



- model equation: since no info was available, it was assumed that the model should be linear ($O_3 = a + b R_s$). The manufacturer gives an equation to transform the voltage output V of the sensor into a mole ratio unit: $O_{3, nmol/mol} = (1000 V - 100)/10$ where V is the sensor responses in V .
- known interference, the manufacturer only mentioned Cl_2 . However looking at the abundance of HCl (that is thought to be more common than Cl_2 in ambient air), it is unlikely that Cl_2 can be present at rural sites in sufficient quantity to interfere. Thus, the effect of Cl_2 on the sensor was not studied.
- Field implementation and comparison with reference method: no info available

The manufacturer gave some information about the short and long term stability and other metrological parameters (repeatability, linearity):

- Full scale: 0-250 ppb
- Limit of detection: 20 ppb
- Repeatability at zero: ± 7 ppb
- Repeatability à 35% of FS : ± 20 ppb
- Linearity $< 10\%$
- Short term drift for zero < 5 ppb/24hr
- Short term drift of sensitivity $< 1\%$ FS/24hr
- Long term drift for zero < 10 ppb/month
- Long term drift of sensitivity $< 2\%$ FS/month
- Rise time (t_{10-90}) < 90 s (180 s with important HR change)
- Fall time (t_{90-10}) < 90 s (180 s with important HR change)
- Effect of interference : Cl about 80 %
- Conditions of use : $20^\circ C$ to $40^\circ C$ / 15 to 90% HR without condensation, 1013 mbar ± 200 mbar
- Diameter : 32 mm - Length : 62mm
- Weight 55g
- Maximum concentration (short time): 50ppm
- Annual limit concentration (average on 1 hr) 780ppm
- Recommended storage: Temperature between $5^\circ C$ and $20^\circ C$, relative humidity 15-90 % without condensation, pressure 1013 ± 200 mbar

Personal communication of the manufacturer: a Membrapor sensor is used in the Cairclip gas sensor.

5 Laboratory experiments

5.1 Exposure chamber for test in laboratory

The gas sensors were evaluated in an exposure chamber. This chamber allows the control of O_3 and other gaseous interfering compounds, temperature, relative humidity and wind velocity (see Figure 3). The exposure chamber is an "O"-shaped ring-tube system, covered with dark insulation material. The exposure chamber can accommodate the O_3 micro-sensors directly inside the "O"-shaped ring-tube system.

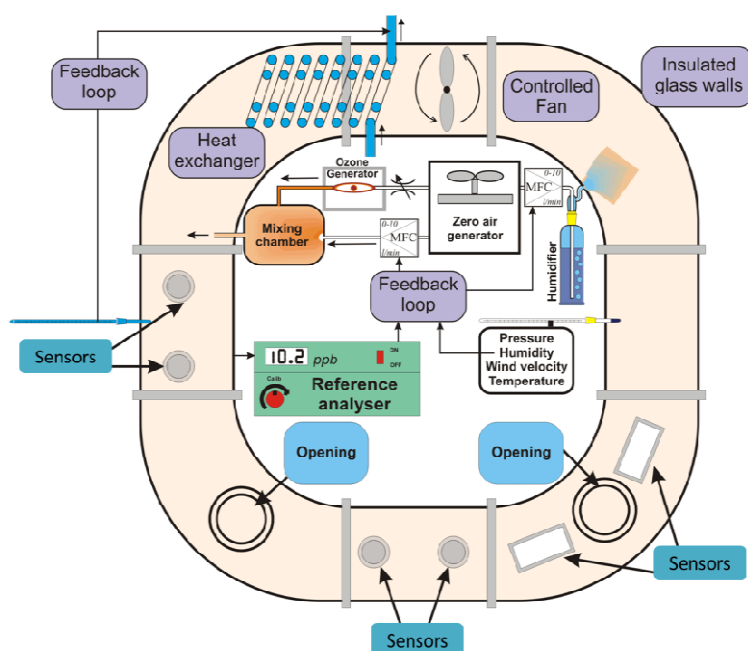


Figure 3: Exposure chamber for micro-sensors used in laboratory

A special Labview software has been developed for controlling the exposure chamber and for easy programming a set of experiments under different controlled conditions: temperature, humidity, wind velocity, O_3 and gaseous interfering compounds. It allows setting criteria for the stability of each parameter and for duration of each step. The software is also able to manage data acquisition so all measurements (reference method plus sensor responses) and exposure conditions were collected in Access database for latter data treatment. The software was able to set initial values for all parameters controlling the generation of gaseous interference, temperature, humidity) according to the targets of meteorological parameters and levels of gaseous compounds. During experiments, an automatic system (feed-back loop) used the reference measurements for gaseous compounds, temperature, humidity and wind speed to auto-correct the gas mixture generation system, temperature controlling cryostat and wind velocity to reach the target conditions (see Figure 4 and the logical graph in Figure 5).

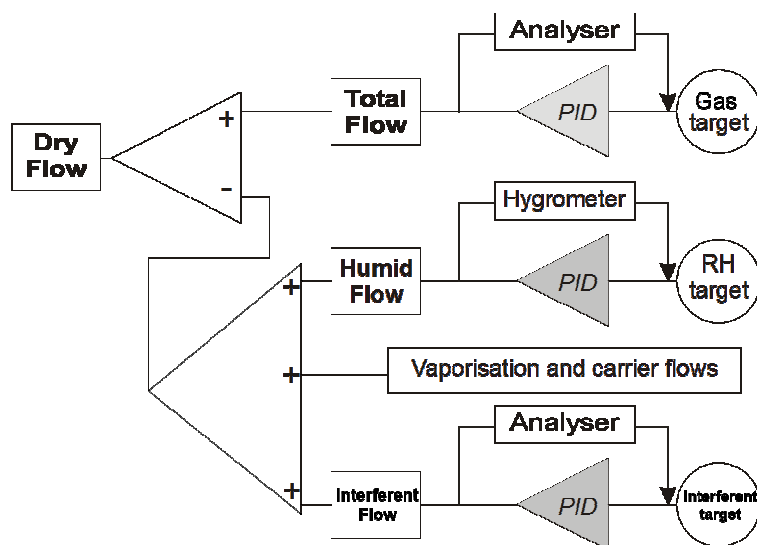


Figure 4: Feedback loop for gaseous compounds and humidity

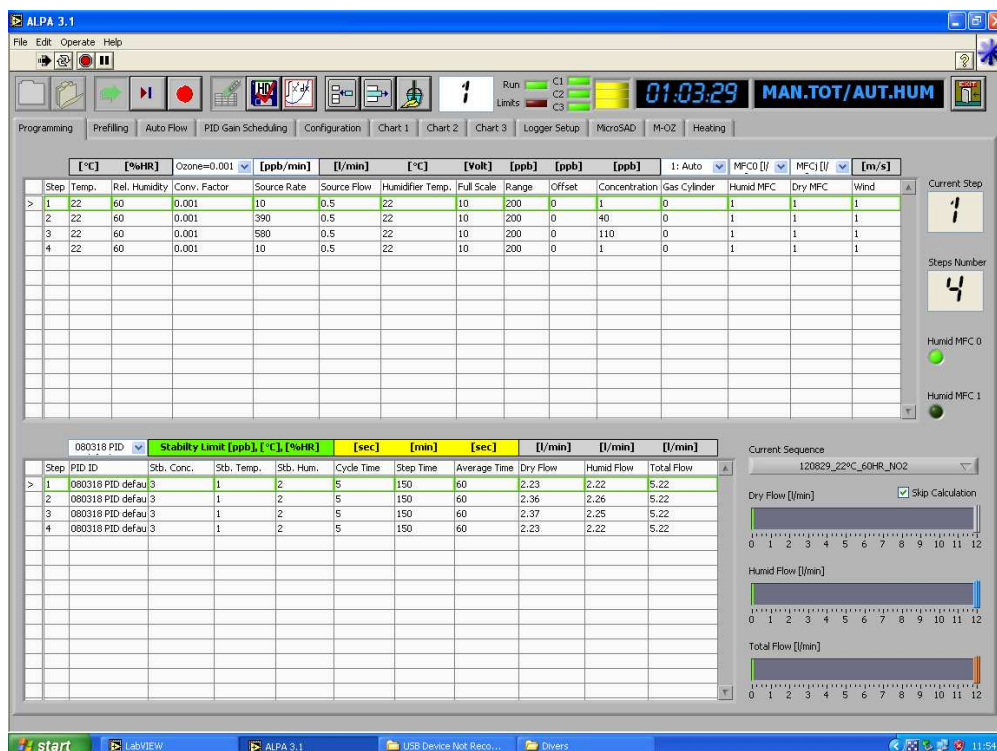


Figure 5: Example of programming of conditions

5.2 Gas mixture generation system

For generating O_3 , two MicroCal 5000 Umwelttechnik MCZ GmbH (G) generators were used. These generators are equipped with UV lamps placed in thermo insulated chamber whose UV beam is controlled by a regulated current intensity. The UV lamp dissociated O_2 molecules into activated O^* atoms that later combined with O_2 molecule to form O_3 . The quantity of O_2 depends on the intensity of the current applied to the UV lamp and the total flow of zero air of the generator which was adjusted by a mass flow controller and controlled by the exposure chamber LabView software. Prior to experiment, the mass flow controllers were calibrated against a Primary Flow Calibrator Gilian Gilibrator 2. The ozone mixtures generated by the MicroCals were calibrated against the NIST primary O_3 photometer of the ERLAP laboratory.

Mixtures of gaseous interference were generated with an in-house designed Permeation system, using NH_3 , NO_2 , SO_2 and HNO_3 permeation tubes from KinTec (G) and Calibrage (F) that were weighed every 3 weeks. CO mixtures were directly generated by dynamic dilution from highly concentrated cylinders from Air Liquide.

For the response time experiment, the controlled conditions in the exposure chamber shall be established after a few minutes. Seen the internal volume of the exposure chamber (about 120 L), it was decided to use the automatic bench that ERLAP uses for the European inter-comparison exercises of the National Reference Laboratories of Air Pollution [6] that can generated mixture with a flow of about 100 L/min.

5.3 Reference methods of measurements

5.3.1 Methods

O_3 was monitored using a Thermo Environment TEI 49C UV-photometer. The analyser was calibrated before the experiments using an O_3 primary standard. It consists of a TEI Model 49 C Primary Standard, Thermo Environmental Instruments cross-checked against a long-path UV photometer (National Institute of Standards and Technology, reference photometer n°4 2, USA).

Other gaseous compounds were recorded to ease understanding sensors results:

6 For example: M. Barbieri and F. Lagler, Evaluation of the Laboratory Comparison Exercise for SO_2 , CO, O_3 , NO and NO_2 , 11th-14th June 2012, EUR 25536, ISBN 978-92-79-26844-1, ISSN 1831-9424, doi:10.2788/52649, ftp://ftp_erlap_ro:3rlapsyst3m@s-jrciprv-ftp-ext.jrc.it/ERLAPDownload.htm



- NO/NO_x/NO₂: Thermo Environment 42 C chemiluminescence analyser, calibrated against a permeation system for NO₂ and a NO working standard consisting of a gas cylinder at low concentration (down to 50 nmol/mol) certified against a Primary Reference Material of NMI VSL - NL.
- SO₂: Environment SA AF 21 M, calibrated with a working standard consisting of gas cylinder at low concentration (down to 50 nmol/mol) certified against a Primary Reference Material of NMI VSL - NL. The calibration of the analyser was confirmed by cross-checking with a permeation method.
- CO: Thermo Environment 48i-TLE NDIR analyser, calibrated with a CO working standard consisting of a gas cylinder at low concentration (down to 50 nmol/mol) certified against a Primary Reference Material of NMI VSL - NL.
- CO₂: an infra Red sensor, Gascard NG 0-1000 µmol/mol (Edinburg Sensors – UK) was used. This sensor includes pressure correction and temperature compensation. The sensor was calibrated with a CO₂ cylinder (369 ppm for Air Liquide) and zero air obtained from an ultra pure Nitrogen cylinder.
- Analyser of NH₃ Ammonia Analyzer, Model 17i (courtesy of monitoring network of Bolzano/Bozen – Italy)

In addition, some other parameters were recorded and/or controlled using:

- 3 Refrigerated/Heating Circulators (Model) were used to regulate the temperature of the exposure chamber. One cryostat was used to control the temperature inside the exposure chamber, another one for the surface of the O-shaped glass tube and the last one was devoted to the control of temperature of the humid and dry air flows. These cryostats used a laboratory calibrated pt-100 probe placed inside the exposure chamber.
- 2 KZC 2/5 sensor from TERSID-It (one with ISO 17025 certificate) were used to control temperature and relative humidity. One sensor was used to monitor in real-time using our Labview software, the second one was used to register these parameter.
- 1 Testo 445 sensor (Testoterm – G) with a temperature and relative humidity probe was used as a control interface to check values inside the chamber.
- 1 Testo 452 sensor (Testoterm – G) with a temperature and relative humidity probe was used as a reference sensor and to monitor temperature and relative humidity.
- 1 wind velocity probes based on hot-wire technology was use to monitor wind velocity during tests.
- 1 pressure gauge DPI 261 from Druck (G) was used to monitor pressure inside the exposure chamber

The sampling line of each gas analyser was equipped with a Naflyon dryer to avoid interference from water vapour on O₃, NO_x, SO₂ and CO analyser

5.3.2 Quality control

During the experiments, the O₃ analyser was monthly checked using a portable O₃ generator SYCOS KTO 3 (Ansyco, GmbH - G) certified against the laboratory primary standard (NIST n°42). The NO₂, SO₂ and CO analyser were calibrated once a month using cylinders certified by the ERLAP laboratory. ERLAP is ISO-17025 accredited (ACCREDIA-IT, n°1362) for the measurement of O₃, NO₂, SO₂ and CO according to EN 14625:2012, EN 14211:2012, EN 14212:2012 and EN 14626:2012, respectively.

5.3.3 Homogeneity

Several tests were performed to confirm the homogeneity of exposure conditions in the chamber at several positions in the exposure chamber. The influence of humidity on the reference analysers was eliminated by using a naflyon dryer. The data acquisition system had a frequency of acquisition of 100 Hz and average over one minute where stored.

6 Metrological parameters

6.1 Response time

The response time of sensors, t_{90} , was evaluated by estimating t_{0-90} and t_{90-0} (the time needed by the sensor to reach 90 % of the final stable value or 0), after a sharp change of test gas level from 0 to 80 % of the full scale (FS) (rise time) and from 80 % of FS to 0 (fall time). Four determinations of rise and fall t_{90} were

performed as shows Table 4. The averaging time of the O₃ TECO 49C analyser was set to 60 sec in order to get a fast response of the reference analyser.

Table 4: Response time measurements

Step	Test gas	RH	T	Interference	Notes
1	90 nmol/mol	60 %	22 °C	none	Until stable response
2	0 nmol/mol	60 %	22 °C	none	Until stable response
3	90 nmol/mol	60 %	22 °C	none	Until stable response
4	0 nmol/mol	60 %	22 °C	none	Until stable response
5	90 nmol/mol	60 %	22 °C	none	Until stable response
6	0 nmol/mol	60 %	22 °C	none	Until stable response
7	90 nmol/mol	60 %	22 °C	none	Until stable response
8	0 nmol/mol	60 %	22 °C	none	Until stable response
9	90 nmol/mol	60 %	22 °C	none	Until stable response

Given that any change of an influencing variable would result in overestimation of t_{90} , these parameters were kept as stable as possible. Table 5 shows that the Relative Standard Deviations (RSD) of temperature, humidity rate, pressure, wind speed and NO₂ were within 1% at FS and lower than 0.5 nmol/mol at zero apart from the 1st step. It was not possible to control ambient pressure. The highest instability in pressure was observed during the Step 8 with a high standard deviation of 0.4 hPa compared to other steps. Table 6 shows in the 1st row the response time of the O₃ analysers that includes both the stabilization time in the exposure chamber and the t_{90} of the analyser itself (about one minute), in the 2nd row the total response time of the sensor and in the third row the response time of the sensor minus the response time of the analyser.

Table 5: Response time experiment, stability of physical parameters during experiments. Temperature is in degree Celsius, relative humidity is in %, pressure is in hPa, O₃, NO₂ and NO are in nmol/mol.

	Step 1	Step 2	Step 3	Step 4	Step 5	Step 6	Step 7	Step 8	Step 9
O ₃ , nmol/mol	92.3±0.75	0.0 ±0.2	91.7±0.2	2.6±0.3	91.7±0.2	-0.5±0.2	91.7±0.3	-0.5±0.2	91.7±0.2
Temperature, °C	22.1±0.01	22.0±0.03	22.1±0.02	22.1±0.02	22.0±0.03	22.0±0.03	22.0±0.02	22.0±0.03	22.0±0.02
Humidity, %	60.0±0.1	59.4±0.9	60.0±0.03	59.9±0.1	60.0±0.03	60.0±0.02	60.0±0.04	60.0±0.02	60.0±0.03
Pressure, kPa	987.4±0.1	998.6±0.3	999.3±0.1	997.9±0.1	1000.3±0.1	1000.7±0.1	1000.3±0.2	998.6±0.4	997.5±0.1
NO ₂ , nmol/mol	0.3±0.4	0.7±0.1	0.7±0.2	1.0±0.1	0.7±0.1	0.7±0.1	0.7±0.2	0.7±0.1	0.7±0.2
NO, nmol/mol	1.9±0.3	1.8±0.1	1.8±0.1	1.8±0.1	1.7±0.1	1.8±0.1	1.8±0.1	1.8±0.1	1.8±0.1
Time length, in min	17	218	150	210	1050	195	180	150	165

Table 6: Sensor's response time (t_{90}) compared to the UV-analyser response time in the exposure chamber for the CairclipO₃/NO₂ sensor. For each sensor, in the 2nd lines, the t_{90} of the O₃ analyser, corresponding to the stabilising in the exposure chamber is subtracted.

t_{0-90} or t_{90-0}	Step 2	Step 3	Step 4 long 90	Step 5	Step 6	Step 7	Step 8	Step 9
	Fall	Rise	Fall	Rise	Fall	Rise	Fall	Rise
O ₃ , UV Photometry	15 min	4 min	5 min	4 min	4 min	4 min	4 min	4 min
CairclipO ₃ /NO ₂	6 min	5 min	6 min	7 min	4 min	7 min	5 min	6 min
CairclipO ₃ /NO ₂ - O ₃	2 min	1 min	1 min	3 min	0 min!	3 min	1 min	2 min

The estimated response times in this experiment were likely slightly underestimated because of the subtraction of the response time of the reference analyser while the sensors started responding before the end of the analyser response time.

The response time of the gas sensor was generally longer than the one of the ozone analyser, excepted for step2 which was not representative since step1 was very short and the flow of the generation system was not sufficient in step 2. In fact, the response time of step 2 is quite different, compared to the rest of the experiment and thus was discarded.

In average, the response time of the Cairclip O₃/NO₂ sensor was about 1 and ½ minutes. As requested in the evaluation protocol [1], the t_{90} of the sensors is less than ¼ of the required averaging time of one hour and the sensors were able to reach stability within the averaging time. Compared to the majority of the tested sensors, the O₃ Cairclip sensor showed a short response time.

In average, the sensor was faster in fall condition (0.7 minute) than in rise condition (2.6 minutes). Even though, this difference exceeds 10 %, it is assumed that it will not affect significantly an hourly average at rural site where ozone concentrations slowly changes.

It is stated that measuring instruments should produce individual measurements that are not influenced by previous individual measurements provided that two individual measurements are separated by at least four response times [8, 3.16]. Therefore, for the following experiments, all steps should last for at least $2.7 \times 4 = 11$ minutes plus the stabilisation time of the exposure chamber. However, because of other slower sensors, it was decided to have each lasting for 150 minutes, well longer than the response time of the Cairclip sensor.

Although it was not the objective of the present project, the Cairclip sensor is fast enough for mobile monitoring, being able to deliver 11 minute averages. However, micro-environment where air pollutants changes with a periodicity of a few minutes (e. g. in front of traffic light or with rapid indoor/outdoor moves) will not allow the sensor to produce independent measurements with this periodicity.

6.2 Pre calibration

The objective of this experiment was to check if the transformation of sensor responses into air pollutant concentration does not include any bias at the mean temperature and relative humidity.

The full scale of the sensor was set to 120 nmol/mol. More test levels were used the following pattern 80, 40, 0, 60, 20, 95% of the full scale. The order of the tests was randomised to take into account possible hysteresis effect (see Table 7). Temperature and humidity, which were suspected to affect the sensor response, were kept under control with relative standard deviation (RSD) of about 1 % while it is not possible to control atmospheric pressure. The temperature and relative conditions of the test were set at 22°C and 60 % of relative humidity, the defined average values.

Table 7: Experimental conditions for pre-calibration experiments of the Cairclip sensors

O ₃ , nmol/mol	NO ₂ , nmol/mol	T, °C	RH, %	Pressure, hPa	Interference	Directive levels
-0.4 ± 0.2	0.3 ± 0.2	22.0 ± 0.03	60.0 ± 0.03	990 ± 0.1	None	
20.1 ± 0.3	0.3 ± 0.4	22.0 ± 0.03	60.0 ± 0.03	990 ± 0.1	None	
41.0 ± 0.2	0.2 ± 0.2	22.0 ± 0.02	60.0 ± 0.03	991 ± 0.1	None	AOT40
61.3 ± 0.2	0.4 ± 0.2	22.0 ± 0.02	60.0 ± 0.04	992 ± 0.2	None	LV
92.0 ± 0.3	0.4 ± 0.1	22.1 ± 0.02	60.0 ± 0.03	991 ± 0.1	None	IT
112.3 ± 0.3	0.4 ± 0.1	22.1 ± 0.02	60.0 ± 0.04	990 ± 0.2	None	AT

The results of the experiment were used to calibrate the sensor (see Figure 6). As a consequence of the curvature of the calibration functions, one can observe flat sensor responses for concentration lower than 40 nmol/mol leading to high uncertainties at low concentration levels.

According to the manufacturer, this behaviour was never observed so far. It should result from a dis-conditioning of the sensor. Every sensor is conditioned in the manufacturer factory before shipment. If a dis-conditioning happens, the sensitivity of the sensor decreases until it is exposed to sufficient O₃ levels. This phenomenon happens when sensors are exposed in laboratory to air without O₃.

However, the sensor was submitted to different levels of O₃ concentration levels without interruption similar to what happens in ambient air when the O₃ goes to zero at night and rise during sunshine. Moreover the same curvature of the sensor responses was observed during 7 calibrations between Aug. and Oct 2012, whether the sensor was submitted to zero air before or not (see Figure 6). Conversely, this curvature was not observed with the field sensor (see Figure 21) (while it is not possible to know if it was maintained conditioned or not). Another possible explanation given by the manufacturer was a possible lack of O₂ in the gaseous mixture in the exposure chamber. However, the laboratory experiments were performed keeping the natural O₂ level of ambient air in the exposure chamber. It was not possible to conclude whether the curvature phenomenon was linked with the sensor behaviour or if it is caused by a data treatment. In the version of the O₃ sensor that we received, we could not avoid the flattening at low concentration whether it was caused by any data treatment or not.

The pre-calibration function was established by plotting sensor responses transformed in O₃ nmol/mol with the equation given in the data sheet (see 4) versus the reference values measured by the TECO 49C analyser (see Figure 6). Each step lasted for 150 minutes once the condition of O₃ concentrations, temperature and humidity were reached. The averages of the last 60 minutes are plotted. The plot at left gives only the initial calibrations and the plot at right shows all the calibration curves between August and October 2012.

The two types of calibrations function could be fitted to experimental data: either a parabolic or a sigmoid model (see Figure 6). The latter equation allowed slight improvement of the residuals of the calibration compared to the parabolic model (Eq. 1 for the initial calibration and Eq. 2 if the whole laboratory experiment).

Observing Figure 6, it appeared that in the range 40 to 80 nmol/mol, the sensor had some type of linear response with slope of 1 but an intercept of 39.9 nmol/mol. However, the residuals of the linear model are correlated with the O₃ reference values. The parabolic and the sigmoid model (see Figure 6) allow removing the dependence of the residuals with the O₃ reference values.

$$\text{Cairclip O}_3/\text{NO}_2, \text{O}_3 = \log\left(\frac{171.0-79.1}{R_s-79.1} - 1\right)/-0.0565 + 85.2 \text{ for } R_s > 79.1 \text{ nmol/mol} \quad \text{Eq. 1}$$

$$\text{Cairclip O}_3/\text{NO}_2, \text{O}_3 = \log\left(\frac{179.0-76.9}{R_s-76.9} - 1\right)/-0.0499 + 88.5 \text{ for } R_s > 76.9 \text{ nmol/mol} \quad \text{Eq. 2}$$

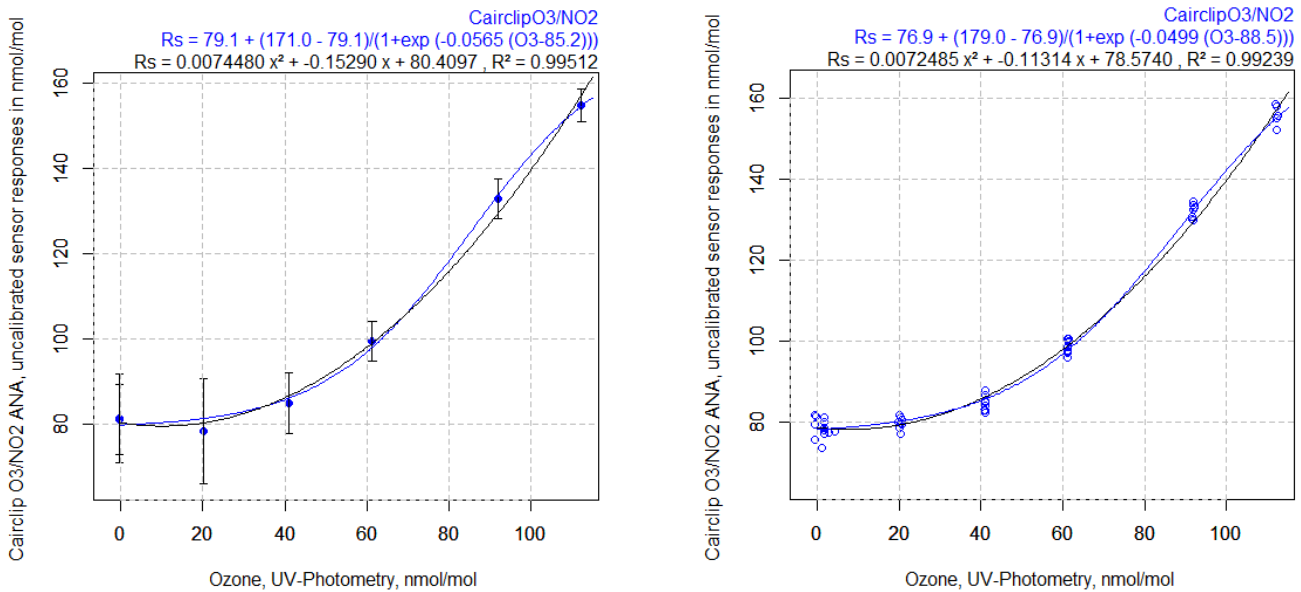


Figure 6: Right: initial calibration of the Cairclip sensors at 227 calibrations between 14- Aug and 07-Oct

For the initial calibration with the sigmoid model, the standard uncertainty of the lack of fit of calibration, $u(\text{lof})$ was estimated using Eq. 3. ρ_{max} is the maximum residual of the model and $u(\text{ref})$ is the uncertainty of the reference measurements set to 1.5 nmol/mol (corresponding to 5 % of relative expanded uncertainty at the LV). If only considering O₃ reference values higher than 40 nmol/mol, ρ_{max} was equal 1.8 nmol/mol resulting in $u(\text{lof})$ found to be equal to 1.8 nmol/mol for the initial calibration of the sensor. Considering all calibrations between August and October 2012, the standard deviation of all residual was 2.1 nmol/mol for. $u(\text{lof})$, calculated using Eq. 4, was found to be equal to 2.6 nmol/mol.

$$u^2(\text{lof}) = \rho_{\text{max,LV}}^2/3 + u^2(\text{ref}) \quad \text{Eq. 3}$$

$$u^2(\text{lof}) = s^2 + u^2(\text{ref}) \quad \text{Eq. 4}$$

In all the cases, $u(\text{lof})$ was small enough to be consistent with the DQO. $u(\text{lof})$ would not be included into the estimation of the laboratory uncertainty since the standard uncertainty of lack of fit of the experimental design/modelling (see 8) would include the standard uncertainty of the lack of fit of the calibration function.

In the tests which follows, this pre-calibration equation was applied before any other data treatment. Eq. 2, the reverse calibration function, was generally applied. However this model could only calculate O_3 for responses lower than 179.0 see Eq. 2. This limit was exceeded when O_3 and NO_2 were at their highest values (115 and 95 nmol/mol). In this case, the parabolic model (see Figure 6 at right) was applied. Because of the curvature of the calibration function and its scattering at zero, it was difficult to apply the calibration function at low values (and sometimes at 20/40 nmol/mol). Consequently, around zero, the calibration function was not used and O_3 was estimated by subtracting the average of all responses of the sensor at 0 nmol/mol to the sensor responses. The curvature of the calibration function between [0;40] nmol/mol decreased the sensor sensitivity, making it difficult to monitor around 20 nmol/mol, the AOT40, an important threshold of the Air Quality Directive at rural areas.

6.3 Repeatability, short-term and long-term drifts

The repeatability, short-term drift and long-term drift of the sensor were determined by calculating the standard deviation of sensor values for 3 consecutive averaging time periods, several consecutive days and from time to time over a longer period (originally planned every 2 weeks during three months).

The repeatability figure imposes limits on the accuracy of the calibration and allowed estimation of the limit of detection and limit of quantification of the sensor. The short term stability was used to set the maximum time between similar tests or the contribution of the short term stability to the measurement uncertainty. The long term stability was used to set the periodicity of recalibration and maximum time between similar tests. If a trend in the long term drift was identified, it would be included into the model equation or later treated as sources of uncertainty.

6.3.1 Repeatability

The repeatability of the sensor responses was calculated using the standard deviation of sensor values for 3 consecutive hourly averages with O_3 being at 0 nmol/mol and 80 % of full scale. All parameters suspected to have an effect on the sensor response (test gas, NO_2/NO , temperature and humidity) were kept under control with relative standard deviation of about 1 %. Each measurement step lasted for the period determined in the response time experiment (see 6). The calculation of the standard deviation of repeatability was carried out using the following equation:

$$s_r = \sqrt{\frac{\sum (R_i - \bar{R})^2}{N - 1}} \quad (\text{Eq. 5})$$

Where R_i is the sensor response for each measurement, \bar{R} is the mean sensor response and N the number of measurements (>3 , see table).

Table 8: repeatability figures at 0 and at 90 nmol/mol of ozone with mean and standard deviation of parameters

		O_3	NO_2	NO	CO	T	Rel. Hum.	P_{hPa}	Cairclip O_3/NO_2
		nmol/mol	nmol/mol	nmol/mol	$\mu\text{mol/mol}$	$^{\circ}\text{C}$	%	hPa	nmol/mol
	Mean $\pm s$ (n=9)	$0.0 \pm 0,1$	$0,7 \pm 0,0$	$1,7 \pm 0,1$	$250 \pm 13,0$	$22,0 \pm 0,0$	$59,1 \pm 0,9$	$993,5 \pm 5,1$	NA
Hourly values	Mean $\pm s$ (n=13)	$91,7 \pm 0,0$	$0,7 \pm 0,0$	$1,7 \pm 0,0$	268 ± 13	$22,0 \pm 0,0$	$60,0 \pm 0,0$	$1000 \pm 0,5$	$91.1 \pm 0,6$
Minutes values	Mean $\pm s$ (n=13)	$91,7 \pm 0,0$	$0,7 \pm 0,0$	$1,7 \pm 0,0$	268 ± 13	$22,0 \pm 0,0$	$60,0 \pm 0,0$	$1000 \pm 0,5$	$91.1 \pm 3,3$

The repeatability figures are given in Table 8. The curvature of the sensor at zero magnified the noise at zero making it impossible to estimate the limit of detection/limit of quantification of the sensor as 3 and 10 times the standard deviation of repeatability at zero.

The repeatability of sensor measurements, the likely difference between two measurements made under repeatability conditions, was computed as $2\sqrt{2}s_r$. s_r was the standard deviation of repeatability of sensor responses when exposed to 90 nmol/mol of O_3 . In average, for hourly values this gives a repeatability of 1.6 nmol/mol for hourly averages. When considering minute values for mobile measurement, this gives a repeatability of 9.2 nmol/mol for hourly averages

6.3.2 Short term drift

For the short term drift, a few measurements were carried out on several consecutive days (in fact with 12 to 36 hours between the first and the second measurements) at 0 nmol/mol, 50 % and 80 % of the LV. The averaging of sensor responses at 0, 60 and 90 nmol/mol were calculated over the last hour of stable conditions of O₃, temperature and relative humidity while each step lasted for 150 min long after stabilisation. The stabilisation of O₃, temperature and relative humidity were reached when the difference between their objective level and actual value was less than 2 nmol/mol for O₃, 1°C and 1 %, respectively. These stabilisation conditions were used throughout this study. The short term stability was estimated using Eq. 6.

$$D_{ss} = \frac{\sum_{i=1}^N |R_{s,after} - R_{s,before}|}{N} \quad \text{Eq. 6}$$

where R_s are the sensor responses (calibrated as in 6.2) at 0, 60 and 90 nmol/mol at t₀ (before) and 24 later (after); N is the number of pairs of measurements. Experiments for which NO₂ or NO were higher than 10 nmol/mol were not considered.

Table 9: Stability of conditions and short term drift of Cairclip sensors with average and standard deviation for each parameter during all experiments.

O ₃ , nmol/mol	NO ₂ , nmol/mol	T, °C	RH, %	Pressure, hPa	Interference	Dss CairclipO ₃
0.8 ± 1.1	0.6 ± 0.2	22.0 ± 0.04	60.0 ± 0.07	994 ± 4.5	None	1.8 ± 1.5 (n=16)
61.2 ± 0.1	0.5 ± 0.2	22.0 ± 0.05	60.0 ± 0.00	990 ± 3.2	None	1.5 ± 0.8 (n=11)
91.8 ± 0.1	0.6 ± 0.2	22.0 ± 0.03	60.0 ± 0.00	995 ± 4.0	None	0.9 ± 0.7 (n=13)

The results of these tests are given in Table 7 and Figure 7 with the number of replicate estimation of Dss at each concentration level.

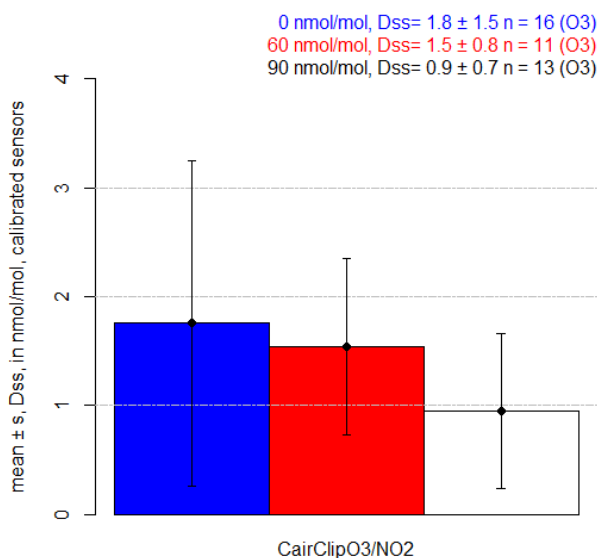


Figure 7: Short term drift for Cairclip sensors at three O₃ levels. Each bar represents the absolute mean differences between Dss at t and t + 24 hours, the errors bars corresponds to the standard deviation of Dss

During the experiments, all parameters suspected to have an effect on the sensor responses (test gas, temperature, humidity test values and other possible influencing) were kept under control. This was necessary to avoid the addition of the scattering of these parameters to the sensor drift. The standard deviation of O₃, NO₂, temperature and humidity are given in Figure 8 which shows low variation with higher level for O₃. The highest variation were found at 0 nmol/mol with 0.9 nmol/mol of O₃ and 0.2 % of relative humidity. As a result, these parameters had negligible influence on the short term stability of the sensors.

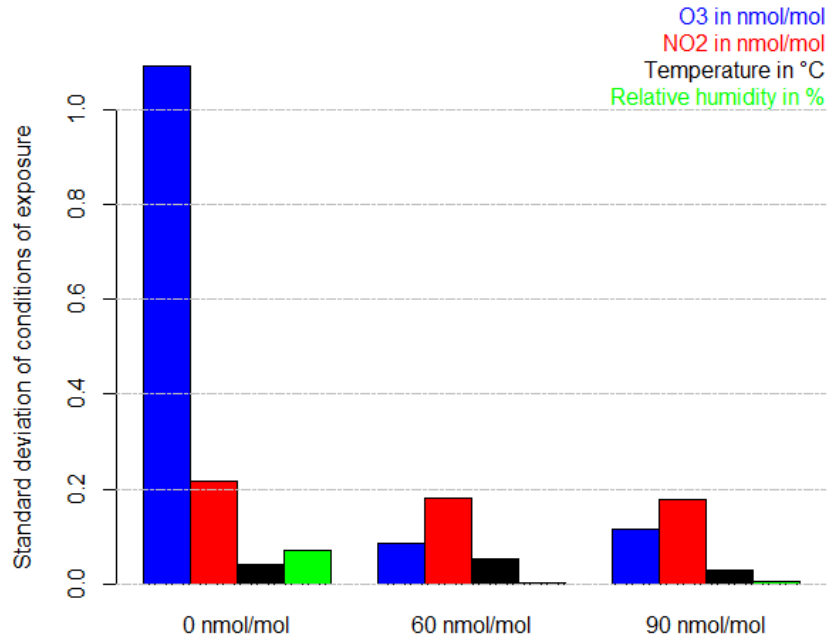


Figure 8: Stability of O₃, NO₂, temperature and humidity in the exposure chamber during the short term drift experiments

The best estimation of the short term drift consists in the average of D_s at 0, 60 and 90 nmol/mol with a contribution to the measurement uncertainty $u(D_{ss})$ calculated using Eq. 7 where s_i represents the standard deviation of the D_{ss} at each concentration level: $D_{ss} = 1.4$ nmol/mol and $u(D_{ss}) = 1.7$ nmol/mol for CairclipO₃/NO₂.

$$u^2(D_{ss}) = \frac{\sum_{i=1}^k (n_i - 1) s_i^2}{\sum_{i=1}^k (n_i - 1)} \quad \text{Eq. 7}$$

In conclusion, since D_{ss} (1.4 nmol/mol) was similar to the repeatability figure (1.6 nmol/mol see 6.3.1), the maximum duration of experiments could be set to 48 hours without risking changes of the sensor responses over time.

6.3.3 Long term drift

For the long term drift, a similar approach was used although over a longer time span. Sensor responses at 0, 60 and 90 nmol/mol were fortnightly measured. The long term drift stability, D_{sl} , was estimated with the same equation as to the short term stability, Eq. 6, except that the differences were estimated between t_0 and the end of all laboratory experiment (90 days).

As for the short drift, the parameters having an effect on the sensor response (O₃, NO₂, temperature, humidity) were kept under control. The standard deviations of O₃, NO₂, temperature and humidity in the exposure chamber are given in Figure 9. It shows good stability for temperature and humidity (less than 0.4 °C and 0.4 %) while the higher figure for O₃ and NO₂ was about 1 nmol/mol. These parameters had no influence on the long term sensor stability.

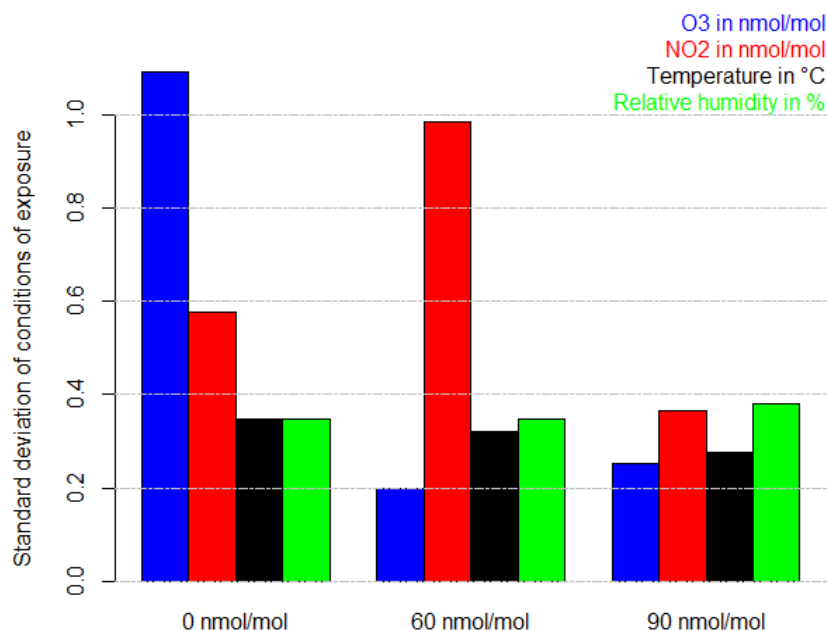


Figure 9: Stability of O₃, NO₂, temperature and humidity in the exposure chamber during the long term drift experiments

Figure 10 shows the long term drift trends, D_{sl} . The sensor shows good stability at 60 and 90 nmol/mol. The slopes of the regression lines are not significantly different from 0, suggesting that the sensor does not undergo any drift. Therefore it was decided not to fit any model correction for the long term drift of the sensor. If found significant, the slopes of the trend lines would suggest, a decrease of the sensor responses of 0.3 and 1.1 nmol/mol for 100 days drift at 60 and 90 nmol of O₃, respectively. The contribution of the long term stability to the measurement uncertainty of sensor measurement $u(D_{is})$ was estimated using Eq. 7 where s_i represents the standard deviation of the sensors response at 0, 60 and 90 nmol/mol; they were found to be 2.2, 1.6 and 1.2 nmol/mol, respectively while $u(D_{is})$ was equal to 1.7 nmol/mol. These figures are slightly higher than the repeatability of the sensor and the short term stability.

In conclusion:

- D_{sl} about 0 with $u(D_{sl}) = 1.7$ nmol/mol. There is no need for correction of the long term drift. Calibration and shelf life: no indication of any need for recalibration or deterioration upon use of the sensor, it was checked by experiment that there is no drift over about 90 days.

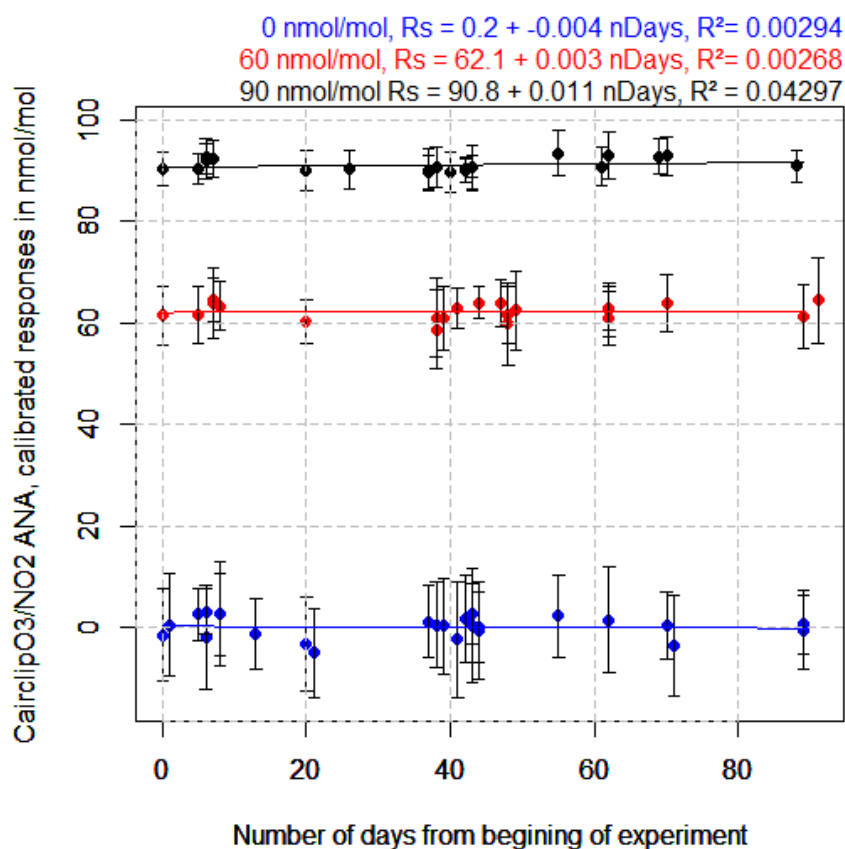


Figure 10: Long term stability of Cairclip sensors

7 Interference testing

7.1 Gaseous interfering compounds

Sensors generally suffer from cross sensibility to other gaseous species that may have a positive or negative effect on the sensor response. According to data in bibliography and the feasibility of generating gaseous mixtures, NO₂, NO, SO₂, CO, CO₂ and NH₃ (see Table 10) were selected for interference testing. The level of the interfering compounds were selected taking into account either the average level of the gaseous interference in the selected micro-environment (see D4.3.1[4]), its maximum value or another more convenient level, which are to be expected to be present in rural ambient air at background sites.

Table 10: Interference testing conditions

	NO ₂ , nmol/mol		NO, nmol/mol		SO ₂ , nmol/mol		CO, μmol/mol		CO ₂ , μmol/mol		NH ₃ , nmol/mol	
level	Low	High(int)	Low	High(int)	Low	High(int)	Low	High(int)	Low	High(int)	Low	High(int)
Compounds	0	~90	0	~100	0		0	8000	Purified air	400	0	± 85
level	Low	High(c _i)	Low	High(c _i)	Low	High(c _i)	Low	High(c _i)	Low	High(c _i)	Low	High(c _i)
O ₃ , nmol/mol	0	~60	0	~60	0	?	0	60	Purified air	60	0	60
Temperature, °C	22		22		22		22		22		22	
Relative humidity, %	60		60		60		60		60		60	

The influence of each interfering compound was determined separately with all influencing variables kept constant during tests. The tests were carried out at the mean temperature and relative humidity and in absence of other interfering compounds. After adjustment of the analyser (the one for measuring O₃ and the one for the interfering compound), the full procedure including four steps was carried out:

- The sensor response Y_0 : the sensor was exposed to the low level of O_3 and without interfering compound;
- The sensor response Y_z : the sensor was exposed to a mixture of zero gas and high level of interfering compound (at int);
- The sensor response c_t : the previous scheme was repeated at a high level of O_3 noted c_t (generally c_t equals the LV) without interfering compounds. The sensor being calibrated, its response generally was equal to c_t the O_3 reference level (otherwise c_t represents the sensor response slightly different from the O_3 reference level);
- The sensor response Y_{ct} : finally the sensor was exposed to a mixture of zero air and high level of O_3 and interfering compounds at the same level as for Y_z (int.).

The mixtures were supplied for a time period equal to one independent measurement, and then, three individual measurement periods (about 150 min). The level of the mixtures of the test gas and gaseous interfering compounds (apart from NH_3 for which we relied on gravimetric values) were measured using reference methods of measurement with a low uncertainty of measurements (uncertainty of less than 5 %) traceable to (inter)nationally accepted standards (see 5.3).

The influence quantity of any interfering compound at zero ($Y_{int,z}$) and at level c_t ($Y_{int,ct}$) are calculated using Eq. 8 and Eq. 9. In Eq. 9, c_t represents the average of the sensor response at concentration c_t of O_3 without interfering compound. The influence quantity of the interfering compound, $Y_{int,LV}$, at the LV of O_3 was calculated using Eq. 10 where C_t is this time the high level of reference O_3 in the exposure chamber measured by UV-photometry. The standard uncertainty associated to the interfering compound, $u(int)$, at the maximum concentration of interfering compound, $C_{i,max}$, was calculated according to Eq. 12 where $C_{i,min}$ is the minimum value of the interfering compound present in the micro environment (see Table 3).

$$Y_{int,z} = Y_z - Y_0 \quad \text{Eq. 8}$$

$$Y_{int,ct} = Y_{ct} - c_t \quad \text{Eq. 9}$$

$$Y_{int,LV} = (Y_{int,ct} - Y_{int,z}) \frac{LV}{C_t} + Y_{int,z} \quad \text{Eq. 10}$$

$$u(int) = \left| \frac{Y_{int,LV}}{int.} \right| \cdot \sqrt{\frac{C_{i,max}^2 + C_{i,max} C_{i,min} + C_{i,min}^2}{3}} \text{ with } u(int) = \left| \frac{Y_{int,LV}}{int.} \right| \cdot \sqrt{\frac{C_{i,max}^2}{3}} \text{ if } C_{i,min} = 0 \quad \text{Eq. 11}$$

$$u(int) = \left| \frac{Y_{int,z}}{int.} \right| \cdot \sqrt{\frac{C_{i,max}^2}{3}} \text{ or } u(int) = \left| \frac{Y_{int,ct}}{int.} \right| \cdot \sqrt{\frac{C_{i,max}^2}{3}} \quad \text{Eq. 12}$$

Because of the oxidation of NO to NO_2 , it was not possible to estimate $Y_{int,z}$ or $Y_{int,ct}$ for NO interfering on O_3 . Moreover, $Y_{int,z}$ may be doubtful because of the flattening of the sensor response at low O_3 levels. In these cases, the simple approach given in paragraph 8.5.6 of ISO 14956:2002 based on the determination of the sensitivity coefficient was applied. The sensitivity coefficient is the difference of sensor responses divided by the extent of the interfering compound level at one level. The table hereafter gives a summary of the effect of all tested interfering compounds. It shows that only NO_2 had a significant effect on the Cairclip sensor, the uncertainty for the rest of the compounds being within the repeatability of the measurements.

Table 11: Summary of results of interference testing for all interfering compounds, the units are the one of the interfering compounds except for the sensitivity coefficient (b) which is in nmol/mol per nmol/mol (or $\mu\text{mol/mol}$ for CO) of the interfering compounds

Interfering compounds	Sensor	Y_0	Y_z	c_t	Y_{ct}	int	$Y_{int,z}$	$Y_{int,ct}$	$Y_{int,LV}$	$C_{i,min}$	$C_{i,max}$	b	u(int)
NO_2 , nmol/mol	CairclipO3/NO2	1.0	97.4	60.1	136.4	90.8	96.4	76.3	76.7	0	40	0.84	19.5
NO, nmol/mol	CairclipO3/NO2	0.4	0.8	63.2	-	99.3	0.6	-	-	0	25	0.006	0.1
CO, $\mu\text{mol/mol}$	CairclipO3/NO2	-	-	61.2	61.7	7.8	-	0.5	-	0	1.5	0.070	0.1
CO_2 , $\mu\text{mol/mol}$	CairclipO3/NO2	1.35	-1.0	77.9	77.9	370	-0.3	0.1	-0.0	350	500	-0.000064	0.0
NH_3 , nmol/mol	CairclipO3/NO2	-	-	61.7	60.9	85	-	-0.8	-	0	170	-0.010	1.0
SO_2 , nmol/mol	CairclipO3/NO2	The sensors were not received at the moment of the tests yet											

7.1.1 Nitrogen dioxide

In this interference test, NO_2 was generated using a permeation system connected to exposure chamber with NO_2 permeation tube. Rapid changes of NO_2 concentration levels were made feasible with a highly concentrated NO_2 cylinders (50 $\mu\text{mol/mol}$) diluted with zero air and controlled by MFC (0-100 mL/min).

The results of the tests are given in Table 12. Y_0 , Y_z , c_t and Y_{ct} refer to the sensor responses in the different interference test levels as explained in 7.1. The responses of the Cairclip sensors are transformed following the pre-calibration function established in the pre-calibration experiment (see 6.2, in this case the parabolic model was used). The controlled conditions (O_3 , NO_2 , T, RH and P) were measured in the exposure chamber during tests. The interference effect and contribution to the measurement uncertainty of the Cairclip sensor are given in Table 11 together with the maximum value and $C_{i,max}$ and $C_{i,min}$ the maximum and minimum values of NO_2 in the selected micro-environment (background station and rural areas, see Table 3).

Table 12: Test conditions for the NO_2 interference testing and sensors responses for the CairclipO3/NO2 sensor. The sensor is pre-calibrated

Date		CairclipO3/NO2, nmol/mol		O_3 , nmol/mol	NO_2 , nmol/mol	T, °C	RH, %	P, hPa
2012-09-11 22:46:52	Y_z	97.4±2.7	c_t	1.0±0.2	89.5±1.2	22.0±0.0	60.0±0.0	992±0.2
2012-09-14 18:16:52	Y_0	1.0±7.1	Y_0	1.6±0.2	0.7±0.3	22.1±0.0	60.0±0.1	985±0.2
2012-10-08 15:53:00	c_t	60.8±9.2	Y_z	61.0±0.7	0.8±0.4	22.6±0.0	60.0±0.1	994±0.2
2012-10-08 18:02:00	Y_{ct}	137.4±2.9	Y_{ct}	61.2±0.4	92.6±4.2	22.6±0.0	60.0±0.0	994±0.1
2012-10-09 05:18:00	c_t	59.4±4.7	Y_z	61.1±0.2	0.8±0.2	22.3±0.0	60.0±0.0	990±0.2
2012-11-03 13:07:30	Y_{ct}	135.4±1.5	Y_{ct}	61.1±0.2	94.8±0.5	22.1±0.0	60.0±0.0	990±0.2

NO_2 is the gaseous component that shows the higher cross-sensitivity with the CairclipO3/NO2. In fact, the sensor was originally designed for the measurement of both NO_2 and O_3 .

When evaluating the interference of NO_2 on the O_3 sensor, it is important to remember that at background site/rural areas, these two pollutants are correlated. In fact, Figure 11 shows the scatter plot between hourly O_3 and NO_2 , all background sites/rural areas in 2008-2009, for the following countries BG, CH, CY, DE, DK, ES, FR, GB, GR, HU, IE, IT, LU, PL, RO, SE, SI with a correlation coefficient of $r=-0.53$.

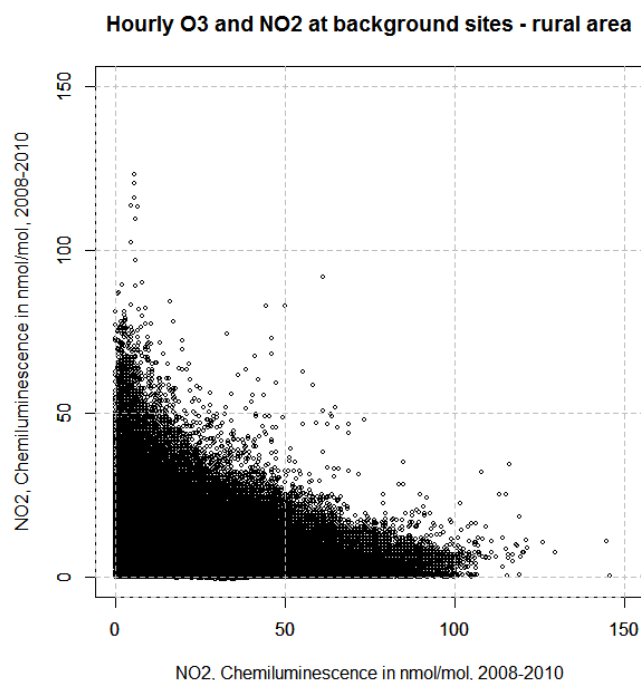


Figure 11: Relationship between hourly O₃ and NO₂, all background sites/rural areas in 2008-2009, for the following countries BG, CH, CY, DE, DK, ES, FR, GB, GR, HU, IE, IT, LU, PL, RO, SE, SI.

7.1.2 Nitrogen monoxide

In this interference test, NO was generated using a highly concentrated NO cylinders (Air Liquide 9468D 62.3 ± 1.2 $\mu\text{mol/mol}$) diluted with the zero air generator of the exposure chamber and controlled by MFC (0-100 mL/min). It was not possible to test the interference of NO, together with O₃ in the exposure chamber which would disappear during the oxidation of NO in NO₂ due to O₃. Consequently, O₃ was kept at about 0 nmol/mol when generating a NO high concentration (see Table 13). The results of the tests are given in Table 13. Y₀, Y_z and ct correspond to the sensor responses in the different interference test levels as explained in 7.1. The responses of the Cairclip sensor were transformed following the calibration function established in the pre-calibration experiment (see 6.2, sigmoid model). The controlled conditions (O₃, NO₂, T, RH and P) are the values measured in the exposure chamber during tests. The interference effect and contribution to the measurement uncertainty of the Cairclip sensor are given in Table 11.

Table 13: Test conditions for the NO interference testing and sensors responses for the CairclipO₃/NO₂. The sensor is pre-calibrated

Date		CairclipO ₃ nmol/mol		O ₃ , nmol/mol	NO, nmol/mol	NO ₂ , nmol/mol	T, °C	RH, %	P, hPa
2012-10-11 18:53	Y ₀	1.0 ± 10.1	Y ₀	-0.5 ± 0.3	1.7 ± 0.1	0.7 ± 0.1	22.4 ± 0.0	60.0 ± 0.0	988 ± 0.1 "
2012-10-11 21:47	ct	63.3 ± 6.7	ct	61.1 ± 0.2	1.7 ± 0.1	0.7 ± 0.1	22.3 ± 0.0	60.0 ± 0.0	988 ± 0.1 "
2012-10-12 10:43	Y ₀	-0.5 ± 9.9	Y ₀	1.0 ± 0.2	1.7 ± 0.1	0.8 ± 0.1	22.2 ± 0.0	60.0 ± 0.0	988 ± 0.1 "
2012-10-12 15:57	Y _z	0.8 ± 11.0	Y _z	-0.7 ± 0.1	101.0 ± 0.2	-0.1 ± 0.4	22.2 ± 0.0	60.0 ± 0.0	987 ± 0.1 "

7.1.3 Carbon monoxide interference

In this interference testing, two CO gaseous mixtures was generated using a highly concentrated CO cylinder (1998 ± 40 $\mu\text{mol/mol}$, Air Liquide-Messer Griesheim 1898G) diluted with zero air of the exposure chamber and controlled by a MFC (0-100 mL/min in a 5 to 20 l/min total flow). The tests were carried out at the mean temperature and relative humidity and in absence of other interfering compounds. After adjustment of the analysers (for O₃ and CO), 2 steps of experiment were carried out: firstly the sensor was exposed to a mixture of zero air and an high level of O₃ ct (60 nmol/mol) and second adding a high level of CO corresponding to the CO limit value of the European air quality directive (8 $\mu\text{mol/mol}$).

The results of the test are given in Table 14 where the columns CairclipO3/NO2 give the calibrated sensor responses, O₃, CO, NO₂, NO, T, RH and P are the values of the conditions in the exposure during tests. The results of this experiment showed that CO had no significant influence on both the O₃ sensor, as one can observe in Table 11 where the uncertainty associated with each interfering compound is given.

Table 14: Test conditions for the CO interference testing and sensors responses for the CairclipO3/NO2. The sensor is pre-calibrated with ozone

Date		CairclipO3 nmol/mol	O ₃ , nmol/mol	CO, nmol/mol	NO, nmol/mol	NO ₂ , nmol/mol	T, °C	RH, %	P, hPa
10-10-12 14:06	Y _{ct}	61.2 ± 8.8	61.1 ± 0.3	8238 ± 19.1	0.8 ± 0.2	1.7 ± 0.1	22.2 ± 0.0	60 ± 0.0	988 ± 0.1"
11-10-12 15:45	ct	61.7 ± 7.5	61.1 ± 0.2	462.5 ± 7.5	0.7 ± 0.1	1.7 ± 0.1	22.6 ± 0.0	60 ± 0.0	988 ± 0.1"

7.1.4 Carbon dioxide interference

The interference tests were carried out at the mean temperature and relative humidity and in the absence of any other variation from other known interfering compounds. In this interference testing, two experiments were carried out: one with air dilution of the zero air of the exposure chamber including CO₂ and one using zero air filtered for CO₂ from a FTIR Purge Gas Generator (85 lpm, Parker-Balston, USA remaining CO₂ lower than 1 µmol/mol). The sensor responses during the two tests were then compared. Target CO₂ levels in the exposure chamber were confirmed using our CO₂ analyser (GasCard NH, Edinburgh Instrument) at the beginning and at the end of the experiment.

The results of the test are given in Table 15. CairclipO3 gives the calibrated sensor responses. O₃, CO₂, CO, NO₂, NO, T, RH and P correspond to the conditions in the exposure during tests. The results of this experiment showed that CO₂ had no significant influence on the O₃ sensor, as one can observe in Table 11 where the uncertainty associated with each interference compound is given. The Ct level corresponds to the experiments at 60 nmol/mol of O₃ of Table 11.

Table 15: Test conditions for the CO₂ interference testing and sensors responses for the CairclipO3/NO2 sensor. The sensor is pre-calibrated

Date		CairclipO3 nmol/mol	O ₃ , nmol/mol	CO ₂ , µmol/mol	CO, µmol/mol	NO ₂ , nmol/mol	NO, nmol/mol	T, °C	RH, %	P, hPa
09-10-12 20:31	Y ₀	1.5 ± 10.4	1.4 ± 10.4	<1	434.3 ± 35.1	0.8 ± 0.2	1.7 ± 0.1	22.3 ± 0.0	60 ± 0.0	989 ± 0.1
09-10-12 23:20	ct	62.6 ± 4.8	62.6 ± 5.2	<1	474.0 ± 8.2	0.8 ± 0.2	1.7 ± 0.1	22.2 ± 0.0	60 ± 0.0	989 ± 0.1
10-10-12 2:22	ct	95.0 ± 5.8	93.2 ± 4.7	<1	466.5 ± 12.9	0.8 ± 0.2	1.7 ± 0.1	22.2 ± 0.0	60 ± 0.0	989 ± 0.1
11-10-12 18:53	Y _z	1.1 ± 10.1	1.0 ± 10.1	~ 370	459.6 ± 7.2	0.7 ± 0.1	1.7 ± 0.1	22.4 ± 0.0	60 ± 0.0	988 ± 0.1
11-10-12 21:47	Y _{ct}	60.2 ± 6.7	63.3 ± 63.9	~ 370	458.7 ± 8.0	0.7 ± 0.1	1.7 ± 0.1	22.3 ± 0.0	60 ± 0.0	988 ± 0.1
12-10-12 0:27	Y _{ct}	94.4 ± 2.3	92.6 ± 9.2	~ 370	457.0 ± 6.4	0.8 ± 0.1	1.7 ± 0.1	22.3 ± 0.0	60 ± 0.1	988 ± 0.1

7.1.5 Sulfur dioxide interference

The sensor arrived too late to be included into the SO₂ interference testing experiment

7.1.6 Ammonia interference

In this interference test, NH₃ was generated using a highly concentrated NH₃ cylinders (Air Liquide 7162F 92.8 ± 2.8 µmol/mol) diluted with the zero air generator of the exposure chamber and controlled by MFC (0-100 mL/min). The tests were carried out at the mean temperature and relative humidity and in absence of other interfering compounds. Two steps were carried out: firstly, the sensor was exposed to a mixture of zero air and O₃ (ct = 60 nmol/mol) and second adding a high level of NH₃.

The results of the test are given in Table 16 where the column CairclipO3 gives the calibrated sensor responses. O₃, CO, NO₂, NO, T, RH and P corresponds to the conditions in the exposure chamber during tests. The results of this experiment showed that NH₃ has no significant influence on the sensors as one can observe in Table 11 where the uncertainty associated with all interfering compound is given.

Table 16: Test conditions for the NH₃ interference testing and sensors responses for the CairclipO₃/NO₂ sensor.
The sensors are pre-calibrated

Date		CairclipO ₃ nmol/mol	O ₃ , nmol/mol	NH ₃ , nmol/mol	CO, μmol/mol	NO, nmol/mol	NO ₂ , nmol/mol	T, °C	RH, %	P, hPa
11-10-12 14:40	ct	61.7 ± 7.5	61.7 ± 0.2	0	463.7 ± 7.5	0.8 ± 0.1	1.7 ± 0.1	22.7 ± 0.0	60 ± 0.0	988 ± 0.2
11-10-12 15:45	Y _{ct}	60.9 ± 6.9	61.1 ± 0.2	85	462.5 ± 7.5	0.7 ± 0.1	1.7 ± 0.1	22.6 ± 0.0	60 ± 0.0	988 ± 0.1

7.2 Air Matrix

The effect of air matrix on the sensor response was tested at all the O₃ levels of the pre-calibration levels (see 6.2). Three different air matrixes were tested: zero air (filtered air), ambient air added to zero air and indoor air added to zero air.

During the experiment, all parameters suspected to have an effect on the sensor response (test gas, temperature, humidity test values and other possible influencing) were kept under strict control with relative standard deviation of about 2 % as shown in Table 17.

For the zero air matrix, the generator of the ERLAP calibration bench (see 5.2) was used. For the two other experiments, a constant air flow, 16.7 l/min, of ambient air and indoor air was injected in the exposure chamber together with zero air.

A low volume sampler (LVS), Derenda 3.1 samplers - G) was used to draw samples from bulk air. Particulate matter was removed from the bulk air using a European PM₁₀ sampling head (EN 12341). The air was sampled just outside our laboratory (nearby a small parking lot) for ambient air and inside our laboratory for the indoor air experiment. The LVS sampling inlets was cleaned before sampling without being greased as requested in EN 12341. The sampling flow of the LVS was adjusted to 1 m³/hr. The target O₃ levels and relative humidity was reached by continuous automatic adjustment of the flows of zero air (dry and humid flows, see the air generator 5.2) before being mixed with the ambient or indoor air constant flow. Therefore the total flow of zero air was different at each experiment. They ranged between 4 and 20 l/min (see Table 17).

As ambient and indoor air sample includes NO₂ molecules which were introduced in the exposure chamber. NO₂ was found to be an interfering compound (see 7.1.1). These NO₂ molecules modified the sensor responses. Consequently, the sensor responses were plotted against the sum of O₃ and NO₂ levels. 84 % of NO₂ was added to O₃, the percentage of NO₂ interference on the sensor. Figure 12 presents the sensor responses for the different air matrixes with and without taking the NO₂ interference taken into account. Three calibration curves were plotted, one only using zero air for dilution, one using a mixture of ambient air and zero air and one using a mixture of indoor air and ambient air. The sensor responses show limited matrix effect with a slight decrease of the intercept/increase of the slope of the regression line for the ambient air/indoor air matrix. These results do not give evidence of any important matrix effect that was not tested in the interference paragraphs.

$$Rs = a + b \cdot c_c \quad \text{Eq. 13}$$

$$c_r = \frac{Rs - a}{b} \quad \text{Eq. 14}$$

$$u_{r,Matrix}^2 = \frac{u(c_r)^2}{c_r^2} = \frac{s_r^2 + s^2(a) + c_r^2 \cdot s^2(b) + 2 \cdot c_r \cdot s(a) \cdot s(b) \cdot r(a,b)}{b^2 \cdot c_r^2} \quad \text{Eq. 15}$$

$$D_{matrix} = \frac{\sum_{i=1}^N |R_{s,matrix} - R_{s,filtered}|}{N} \quad \text{Eq. 16}$$

A weighted linear model (Eq. 13, each weight corresponded to the multiplicative inverse of the variance) was fitted for each type of dilution air: zero air, ambient air and indoor air (see Figure 12) where, Rs was the calibrated response of the sensor (6.2), a and b represented the intercept and the slope of the linear model

and c_c the reference measurements of the test gas. Then Eq. 14 allows determining c_r , the corrected sensor response calculated using Eq. 12. Eq. 15 gave $u_{r,Matrix}$, the relative combined uncertainty due to the air matrix effect where s_r was the repeatability of the sensor response (see 6.3.1) and s denoted the standard deviation of the intercepts (a) and slopes (b). $s(a)$ and $s(b)$ were determined using their scattering in the three linear models for zero air, ambient air and indoor air dilution. The last element of Eq. 15 gave a decrease of uncertainty due to the correlation of the slopes and intercepts ($r(a,b) = -1$). $u_{r,Matrix}$ is given in Figure 12 with value lower than 1.8 % at the O_3 limit value corresponding to 1.1 nmol/mol. The contribution of the matrix effect to the measurement uncertainty is more important at low O_3 levels.

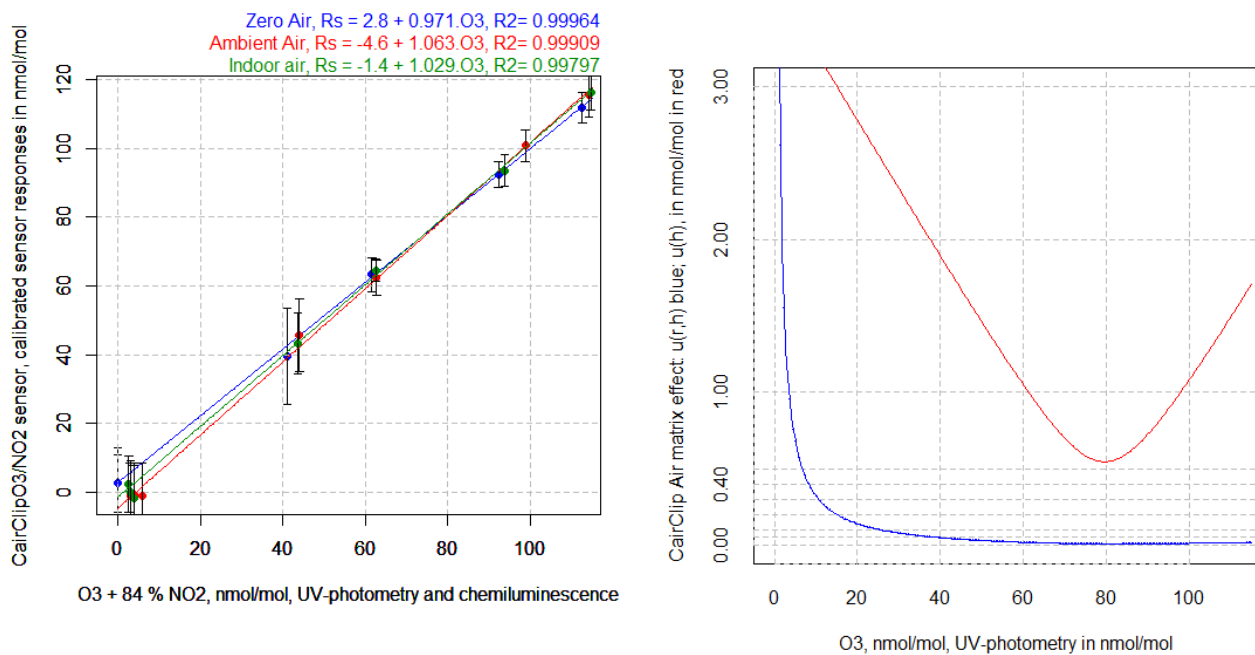


Figure 12: Effect of air matrix on CairclipO3/NO2 sensors. Contribution of the matrix effect to the measurement uncertainty (relative and absolute) of the sensor

Table 17: Stability of exposure conditions and matrix effect of Cairclip sensors with average and standard deviation for each parameter.

O ₃ in nmol/mol	NO ₂ in nmol/mol	T in °C	RH in %	Pressure in hPa	CairclipO3	Zero Air (l/min)	Notes
92.0 ± 0.3	0.4 ± 0.1	22.1 ± 0.02	60.0 ± 0.03	991 ± 0.1	94.3 ± 4.6	8.2	Filtered air
41.0 ± 0.2	0.2 ± 0.2	22.0 ± 0.02	60.0 ± 0.03	991 ± 0.1	38.2 ± 7.0	19.6	
-0.4 ± 0.2	0.4 ± 0.1	22.1 ± 0.02	60.0 ± 0.02	990 ± 0.1	2.6 ± 8.2	10.7	
61.3 ± 0.2	0.4 ± 0.2	22.0 ± 0.02	60.0 ± 0.04	992 ± 0.2	60.3 ± 4.6	16.5	
20.1 ± 0.3	0.3 ± 0.4	22.0 ± 0.03	60.0 ± 0.03	990 ± 0.1	23.2 ± 12.4	15.2	
112.3 ± 0.3	0.4 ± 0.1	22.1 ± 0.02	60.0 ± 0.04	990 ± 0.2	111.3 ± 3.8	7.3	
91.7 ± 0.3	2.6 ± 0.2	22.0 ± 0.03	60.0 ± 0.04	995 ± 0.3	95.4 ± 5.6	10.7	Indoor air (16.7 l/min)
41.0 ± 0.2	3.1 ± 0.5	22.1 ± 0.02	60.0 ± 0.05	995 ± 0.1	41.1 ± 4.6	13.9	
1.7 ± 0.2	1.7 ± 0.5	22.0 ± 0.02	60.0 ± 0.02	993 ± 0.1	-0.1 ± 9.2	19.2	
61.1 ± 0.2	1.8 ± 0.5	21.9 ± 0.02	60.0 ± 0.03	996 ± 0.1	61.7 ± 3.1	16.3	
21.0 ± 0.6	7.1 ± 1.1	22.0 ± 0.04	60.8 ± 0.59	995 ± 0.1	19.3 ± 9.4	11.3	
112.0 ± 0.3	3.2 ± 0.5	22.0 ± 0.03	60.0 ± 0.04	995 ± 0.2	114.0 ± 3.8	5.2	
91.8 ± 0.5	8.3 ± 0.6	22.6 ± 0.02	60.0 ± 0.08	998 ± 0.1	102.5 ± 5.2	11.3	Outdoor air (16.7 l/min)
41.0 ± 0.2	3.6 ± 0.6	22.5 ± 0.02	59.9 ± 0.12	998 ± 0.1	43.0 ± 6.2	8.3	
1.8 ± 0.3	2.5 ± 0.5	22.3 ± 0.02	59.6 ± 0.23	996 ± 0.1	-0.7 ± 9.2	9.3	
61.1 ± 0.3	1.9 ± 0.7	22.3 ± 0.03	60.0 ± 0.04	996 ± 0.1	59.1 ± 4.7	9.3	
19.8 ± 0.3	2.8 ± 0.5	22.3 ± 0.02	60.0 ± 0.02	995 ± 0.1	27.0 ± 6.1	4.1	
112.1 ± 0.2	2.5 ± 0.5	22.2 ± 0.02	60.0 ± 0.04	994 ± 0.2	113.6 ± 4.9	8.4	

7.3 Hysteresis

Hysteresis is the dependence of a system not only on its current environment but also on its past environment. This dependence arises because the system can be in more than one internal state. If a given input alternately increases and decreases, the output tends to form a loop.

The estimation of the dependence of sensors toward hysteresis was carried out by testing a ramp of rising O₃ levels (0, 20, 40, 60, 80, 95% of FS), followed with a ramp of decreasing levels and finally repeating the initial ramp as shown in Table 18. Each point corresponds to the hourly average for one O₃ level at the mean temperature and mean relative humidity.

Table 18: Stability of conditions during the experiments for the determination of hysteresis effect

O ₃ in nmol/mol	NO ₂ in nmol/mol	T in °C	RH in %	Pressure in hPa	CairclipO3	Notes
-0.5 ± 0.2	0.4 ± 0.1	22.0 ± 0.03	60.0 ± 0.02	989 ± 0.2	3.1 ± 4.5	Rise
20.1 ± 0.3	0.4 ± 0.1	22.0 ± 0.03	60.0 ± 0.04	991 ± 0.1		
40.7 ± 0.3	0.4 ± 0.3	22.0 ± 0.03	60.0 ± 0.03	991 ± 0.1	29.1 ± 6.5	
61.3 ± 0.2	0.4 ± 0.4	22.0 ± 0.02	60.0 ± 0.04	991 ± 0.1	63.6 ± 6.8	
91.9 ± 0.2	0.2 ± 0.3	22.0 ± 0.03	60.0 ± 0.04	992 ± 0.2	91.0 ± 4.4	
112.4 ± 0.3	0.4 ± 0.2	22.1 ± 0.02	60.0 ± 0.06	992 ± 0.1	113.6 ± 4.3	
91.9 ± 0.3	0.4 ± 0.2	22.0 ± 0.02	60.0 ± 0.04	991 ± 0.2	91.8 ± 4.3	Fall
61.3 ± 0.2	0.4 ± 0.1	22.0 ± 0.02	60.0 ± 0.04	990 ± 0.2	64.2 ± 4.1	
41.0 ± 0.4	0.4 ± 0.1	22.0 ± 0.03	60.0 ± 0.06	989 ± 0.1	37.6 ± 5.7	
20.3 ± 0.3	0.4 ± 0.2	22.0 ± 0.03	60.0 ± 0.06	990 ± 0.1		
-0.4 ± 0.2	0.3 ± 0.2	22.0 ± 0.03	60.0 ± 0.03	990 ± 0.1	2.7 ± 10.4	
20.1 ± 0.3	0.3 ± 0.4	22.0 ± 0.03	60.0 ± 0.03	990 ± 0.1		
41.0 ± 0.2	0.2 ± 0.2	22.0 ± 0.02	60.0 ± 0.03	991 ± 0.1	3.7.7 ± 7.0	Rise
61.3 ± 0.2	0.4 ± 0.2	22.0 ± 0.02	60.0 ± 0.04	992 ± 0.2	63.1 ± 4.6	
92.0 ± 0.3	0.4 ± 0.1	22.1 ± 0.02	60.0 ± 0.03	991 ± 0.1	91.4 ± 4.6	
112.3 ± 0.3	0.4 ± 0.1	22.1 ± 0.02	60.0 ± 0.04	990 ± 0.2	112.7 ± 3.8	

Figure 13 presents the sensor responses. Three lines are plotted, one for the 1st ramp of rising O_3 levels, one for the 2nd one with falling levels and one for the 3rd ramp of rising levels. The sensor shows minor hysteresis effect with a slight change of the intercept and slope of the regression line. A weighted linear model (Eq. 13) was fitted for each ramp of O_3 levels (see Figure 13) where, R_s was the calibrated response of the sensor (see 6.2, using Eq. 2), a and b were the intercept and the slope of the linear model and c_c the reference O_3 measurements. Then Eq. 14 allowed determining c_r , the corrected sensor response calculated using Eq. 12. Eq. 15 gave $u_{r,h}$, the relative combined uncertainty due to the hysteresis effect where s_r was the repeatability of the sensor response (evaluated in 6.3.1) and s denoted the standard deviation of the slopes (b) and intercepts (a). $s(a)$ and $s(b)$ were determined using their scattering in the linear lines of each ramp of O_3 concentration levels. In the case of hysteresis the correlation between the slopes and intercepts in Eq. 15 was not relevant. The relative standard uncertainty due to hysteresis effect, $u_{r,h}$, is given in Figure 13, left and shows value lower about 1.2 % for O_3 higher than 60 nmol/mol corresponding to a contribution of hysteresis to standard uncertainty of about 0.7 nmol/mol.

The residuals at 40 nmol/mol that can be observed on Figure 13 were caused by the curvature of the calibration. They were higher at 20 nmol/mol so that this reference level was discarded to avoid confounding the curvature effect with the hysteresis effect. By using weighted regression analysis, each weight being to the multiplicative inverse of the variance, the influence of the residuals at 40 nmol/mol was avoided.

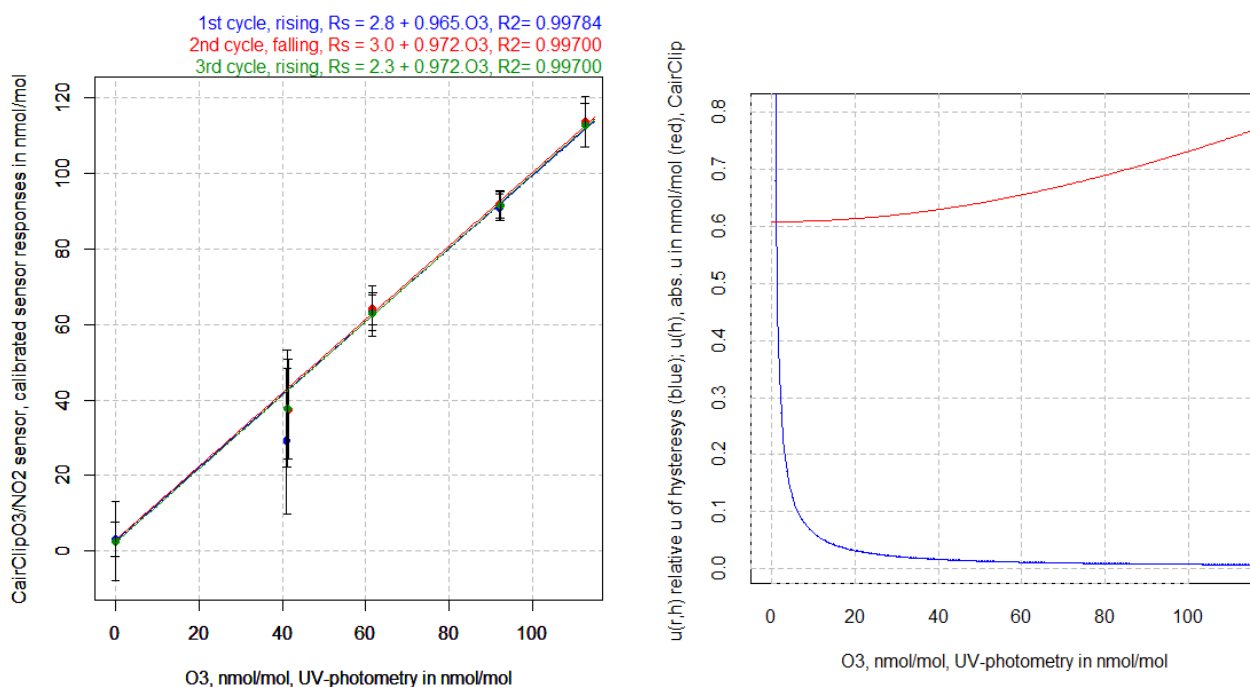


Figure 13: Right: effect of hysteresis on ClairClip sensors showing the response of the sensor in a hysteresis cycle. Left: relative and absolute contribution of the hysteresis effect to the measurement uncertainty of the sensor

7.4 Meteorological parameters

7.4.1 Temperature and humidity

Sensor's response can also be influenced by variation of temperature or relative humidity. To evaluate these effects, we carried out two series of test, generating ramps of temperature and humidity while O_3 and other significant parameters (the sole NO_2) remained under strict control. The ranges of temperature changed between 12 and 32 °C (by step of 5 °C) and the range of humidity was kept between 40% and 80% (by step of 10%), as shown on Figure 14.

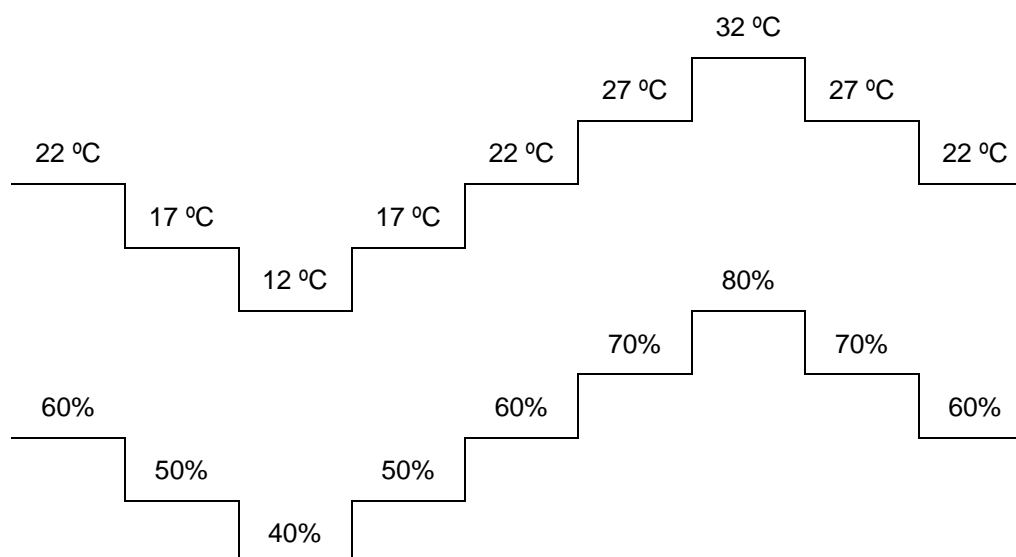


Figure 14: Ranges of meteorological interference

Other parameters suspected to have an effect on the sensor response (test gas, O₃, temperature or humidity) were kept under control with relative standard deviation of about 2 %, see Figure 15 and Table 19. Each step lasted for 150 minutes once the target O₃ concentrations, temperature and humidity were reached. The averages of the last 60 minutes were used to compute the average step responses. The calibration established in 6.2 (Eq. 2) was applied.

Table 19: Stability of exposure conditions and matrix effect of Cairclip sensors with average and standard deviation for each parameter

T in °C	RH in %	Pressure in hPa	O ₃ in nmol/mol	NO ₂ in nmol/mol	CairclipO ₃	Interference	Notes
22.1 ± 0.0	60.0 ± 0.0	986 ± 0.1	61.1 ± 0.3	0.7 ± 0.6	59.5 ± 7.4	None	Increasing temperature
27.2 ± 0.0	60.0 ± 0.0	987 ± 0.1	61.1 ± 0.3	0.7 ± 0.6	60.4 ± 4.5	None	
32.1 ± 0.0	60.0 ± 0.0	987 ± 0.1	61.1 ± 0.3	0.7 ± 0.2	63.1 ± 6.2	None	
27.2 ± 0.0	60.0 ± 0.0	986 ± 0.1	61.1 ± 0.3	0.7 ± 0.1	61.7 ± 5.2	None	Decreasing temperature
22.1 ± 0.0	60.0 ± 0.0	986 ± 0.1	61.1 ± 0.3	0.7 ± 0.3	61.4 ± 5.1	None	
17.2 ± 0.1	60.0 ± 0.0	986 ± 0.1	61.1 ± 0.2	0.7 ± 0.2	60.1 ± 4.6	None	
11.9 ± 0.1	60.0 ± 0.0	986 ± 0.1	61.1 ± 0.3	0.7 ± 0.5	56.7 ± 5.3	None	
16.7 ± 0.0	60.0 ± 0.0	985 ± 0.1	61.1 ± 0.3	0.7 ± 0.5	58.9 ± 5.7	None	Increasing temperature
21.9 ± 0.0	60.0 ± 0.0	986 ± 0.1	61.2 ± 0.3	0.8 ± 0.5	62.3 ± 7.4	None	
22.0 ± 0.0	59.9 ± 0.0	997 ± 0.1	61.2 ± 0.2	0.7 ± 0.1	63.7 ± 2.9	None	Increasing humidity
22.0 ± 0.0	69.9 ± 0.1	984 ± 0.2	61.1 ± 0.2	0.7 ± 0.2	60.4 ± 6.2	None	
22.1 ± 0.0	78.6 ± 0.1	982 ± 0.1	61.1 ± 0.3	0.7 ± 0.2	60.7 ± 7.7	None	
22.2 ± 0.0	70.0 ± 0.1	983 ± 0.1	61.1 ± 0.2	0.7 ± 0.1	63.1 ± 4.8	None	Decreasing humidity
22.1 ± 0.0	60.0 ± 0.0	983 ± 0.3	61.1 ± 0.2	0.7 ± 0.1	63.5 ± 4.5	None	
22.1 ± 0.0	50.0 ± 0.0	984 ± 0.1	61.2 ± 0.3	0.7 ± 0.3	62.9 ± 4.2	None	
22.1 ± 0.0	40.0 ± 0.1	985 ± 0.1	61.1 ± 0.3	0.7 ± 0.3	61.1 ± 5.7	None	
22.1 ± 0.0	50.0 ± 0.0	985 ± 0.2	61.2 ± 0.3	0.7 ± 0.4	59.1 ± 5.5	None	Increasing humidity
22.1 ± 0.0	60.0 ± 0.0	986 ± 0.1	61.1 ± 0.3	0.7 ± 0.6	59.5 ± 7.4	None	

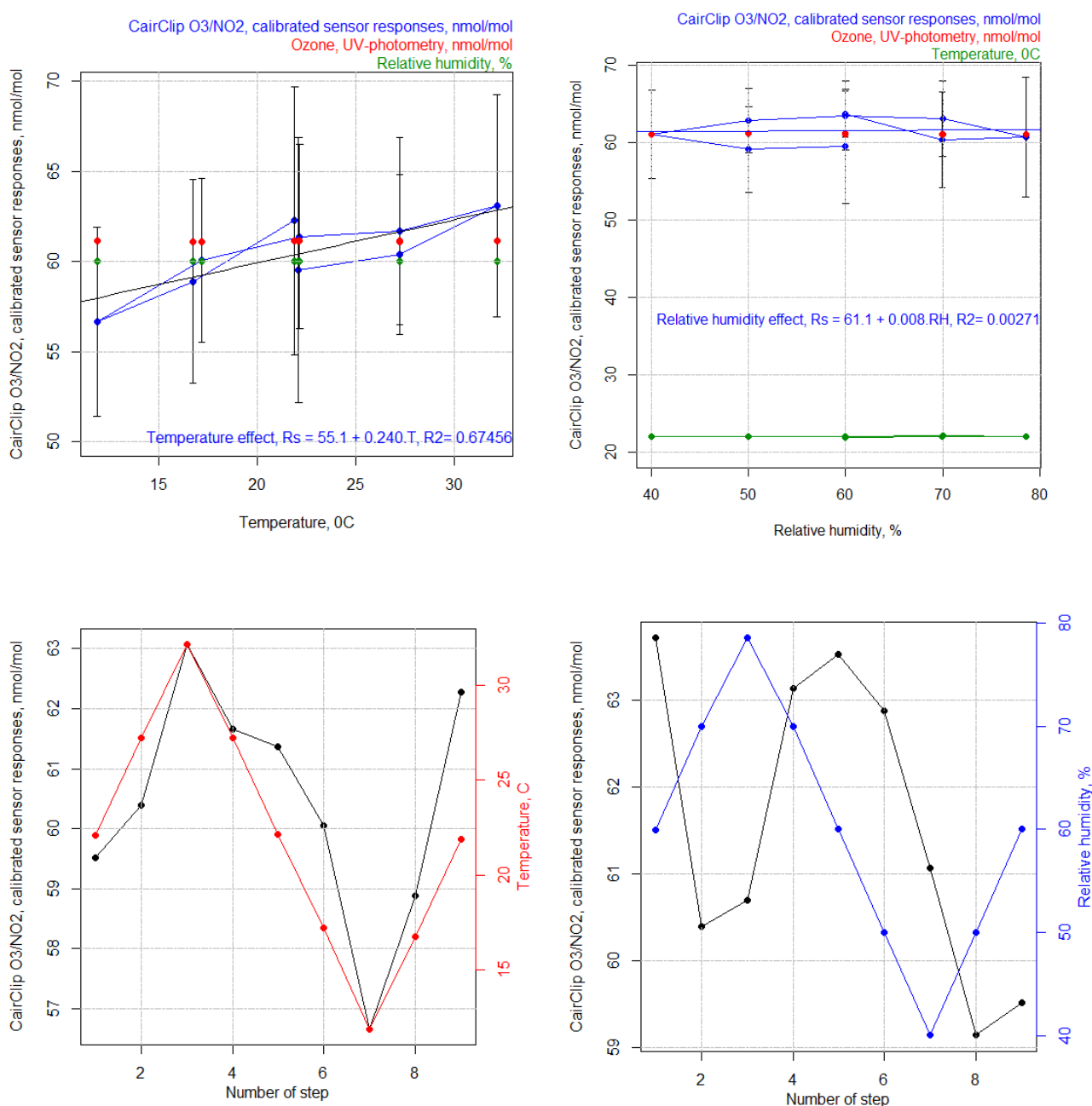


Figure 15: Sensitivity of CairClip O₃/NO₂ sensor toward relative humidity (left) and temperature (right). The error bars give the standard deviations of the sensor responses during the last hour of each test levels

The influences of temperature and humidity on the sensor responses are shown in Figure 15. In average, the sensor did not show any sensitivity to relative humidity (the slope of the regression line being insignificantly different from 0 (actual value: 0.0077 ± 0.055)). Regarding temperature, the sensor showed a slight significant dependence with a slope equal to 0.24 ± 0.04 . The sensor's response increased with temperature. Moreover, a slight hysteresis effect was observed (see Figure 15 and detailed values in Table 15) for the humidity effect. In fact, the sensor responses showed a delay from test level to test level. For example, the sensor responses kept on increasing one step after the maximum temperature/humidity and conversely. The variation of the sensor response against temperature and relative humidity was estimated with Eq. 17 using the sensitivity coefficient b , the slope of the regression lines, to estimate the standard uncertainty, u_x . A



contribution of the hysteresis of temperature and humidity was added. These contributions were set to the maximum deviation or the regression lines.

$$u(x) = \left(b^2 \frac{(X_{\max} - X_{\min})^2}{3} + \frac{\rho_{\max, LV}^2}{3} \right)^{1/2} \quad \text{Eq. 17}$$

Where x is the tested parameter, b is the slope of the regression line of the sensor responses versus temperature and humidity, X_{\max} and X_{\min} the maximum and minimum values encountered in real ambient for parameter x and ρ_{\max} is the maximum residuals between the regression line and the sensor responses or the one at the LV.

Assuming a temperature range between 15 and 45 °C, the maximum residual of the linear fit being 3.3 nmol/mol, the contribution of the temperature effect was $u(T) = 1.9$ nmol/mol with correction of the sensor for the temperature effect or $u(T) = 4.6$ nmol/mol without correction of the sensor for the relative humidity effect.

Assuming a relative humidity range between 30 and 95 %, the maximum residual of the linear fit being 2.3 nmol/mol, the contribution of the relative humidity effect was $u(RH) = 1.4$ nmol/mol. The slope of the regression line was not significant and it was not taken into account.

7.4.2 Wind velocity effect

A test for wind speed ranging between 0.8 and 5 m/s of wind velocity was performed. However, the Cairclip sensor or its data acquisition system did not work correctly during the experiment (sensor responses were negative likely because the internal battery was not powered during this test). An indirect evaluation of the effect of wind velocity was performed by plotting the responses of the long drift experiment at 60 and 90 nmol/mol versus the wind velocity during these tests that show some variation (see Figure 16). The slope of trend line could be used as the sensitivity coefficient of the sensor responses to wind velocity. The observed figures appeared overestimated (-3.8 and -1.6 nmol/mol per m/s of wind velocity at 90 and 60 nmol/mol, respectively). In fact, this experiment includes a few shortcomings: extrapolation due to the limited range of wind velocities with differences between sensor responses being only slightly higher than the repeatability of results. Moreover, a few covariates were not independent (these tests were drawn from the results of other experiments: drift estimation, power supply ...). A range of variation of wind velocity of 0 to 5 ms would lead to a standard uncertainty of 7.5 nmol/mol. This high value was rather unlikely. In fact, we assumed that the changes observed in this experiment were coming from dependent covariates instead of wind velocity.

When reporting these results, the manufacturer informed that the wind effect strongly depends on the direction of the wind and the precise positioning of the sensor whose microfan can be disturbed. Cairpol recommends using their sensor protective box called Cairbox.

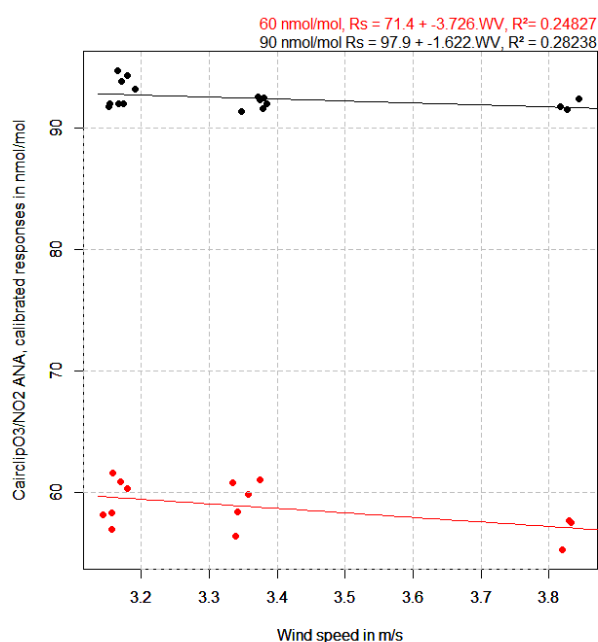


Figure 16: Effect of Wind speed of the sensor responses at 60 and 90 nmol/mol

7.5 Effect of change of ambient pressure

The effect of pressure on the sensor responses was tested at 2 levels of ambient pressure (about ± 10 hPa) while other parameters remained constant: O_3 at the LV, mean temperature and pressure without NO_2 . The change of pressure was obtained by:

- first increasing the dilution flow of the generation system of the exposure chamber while carefully eliminating of possible leak of the glass chamber in order to increase ambient pressure
- and second by decreasing the same dilution flow and increasing the aspiration of the output venting of the chamber in order to decrease ambient pressure without allowing for air sample entering into the chamber, e. g. through openings of the chamber.

Anyhow, the strategy consisting of changing the injection flow was constrained by the need for flow adjustment to reach the target levels of O_3 , NO_2 , temperature, relative humidity and wind velocity. Therefore only a little change of ambient pressure equal to 10 hPa pressure (see Table 20) could be achieved. The results of the test are given in Table 20. During the experiment, O_3 , NO_2 , temperature and humidity were kept constant as much as possible.

Table 20: Effect of change of Pressure on the CairClip sensor responses and conditions of exposure with average and standard deviation for each parameter

Date	Pressure in hPa	T in °C	RH in %	NO_2 in nmol/mol	O_3 in nmol/mol	Cairclip O_3	Notes
17-10-12 17:09	1009 ± 0.3	22.5 ± 0.0	48.6 ± 0.2	4.4 ± 0.7	61.1 ± 1.0	67.1 ± 4.4	High Pressure
17-10-12 18:06	1001 ± 0.1	22.4 ± 0.1	48.9 ± 0.1	5.2 ± 1.4	61.1 ± 0.5	69.7 ± 3.4	Low Pressure
18-10-12 15:05	996 ± 0.1	22.3 ± 0.0	50.0 ± 0.1	3.9 ± 0.9	49.0 ± 1.3	52.3 ± 5.1	Low Pressure
18-10-12 17:06	1006 ± 0.1	22.3 ± 0.0	50.0 ± 0.1	3.8 ± 1.1	47.8 ± 0.3	55.7 ± 6.1	High Pressure

Eq. 18 and Eq. 19 were applied to estimate the sensitivity coefficient of the sensors to change of pressure and the contribution of this parameter to the measurement uncertainty, $u(P)$. In these equations X_n was the tested ambient pressure level, with sensor response C_{X_n} at X_n , X_{max} and X_{min} , the max and min values encountered in real ambient for ambient pressure.

For the mean of the two O_3 levels, the sensitivity coefficient was found to be 0.0411 nmol/mol/hPa and assuming a pressure change in the range of 30 hPa gave a standard uncertainty, $u(P)$, of 1.2 nmol/mol. This latter value being similar to the short term drift, it was likely insignificant.

7.6 Effect of change in power supply

The effect of power supply on the sensor responses was tested at 3 levels of voltage (210, 220 and 230 V) while other parameters remaining constant: O₃ at the LV, and mean temperature and pressure without NO₂. O₃, NO₂, temperature and humidity were kept as constant as possible during the experiment. In this experiment, the power supply of the sensor was changed using a variable rheostat, model Rheothor ADB RT 10 27/B. The results of the test are given in Table 20.

Table 21: Effect of change of power supply on the Cairclip sensor responses and conditions of exposure with average and standard deviation for each parameter

Date	Voltage	T in °C	RH in %	Pressure in hPa	O ₃ in nmol/mol	NO ₂ in nmol/mol	CairclipO3
06-11-12 16:00	220 V	22.3 ± 0.1	60.0 ± 0.1	991 ± 0.3	61.1 ± 0.2	4.9 ± 0.3	63.7 ± 7.4
06-11-12 17:00	230 V	22.2 ± 0.0	60.0 ± 0.1	992 ± 0.2	61.1 ± 0.2	5.0 ± 0.3	64.6 ± 6.9
06-11-12 17:31	210 V	22.2 ± 0.1	60.0 ± 0.1	992 ± 0.2	61.1 ± 0.2	4.9 ± 0.2	55.9 ± 8.2
07-11-12 11:20	210 V	22.1 ± 0.1	60.0 ± 0.1	1003 ± 0.1	61.1 ± 0.2	5.0 ± 0.3	58.3 ± 9.4
07-11-12 13:18	230 V	22.1 ± 0.1	60.0 ± 0.1	1002 ± 0.1	61.2 ± 0.3	5.0 ± 0.4	63.7 ± 7.9
07-11-12 17:20	220 V	22.1 ± 0.1	60.0 ± 0.1	1003 ± 0.3	61.1 ± 0.2	4.7 ± 5.5	64.2 ± 8.4

Eq. 18 and Eq. 19 were applied to estimate the sensitivity coefficient of the sensors to changes of power supply and the contribution of this parameter to the measurement uncertainty of the sensor, $u(X_p)$. In these equations X_n is the tested ambient voltage level, with sensor response C_{X_n} at X_n , X_{\max} and X_{\min} the max and min values expected voltage in field operation.

$$\frac{\Delta C}{\Delta X} = \left| \frac{C_{X_2} - C_{X_1}}{X_2 - X_1} \right| \quad \text{Eq. 18}$$

$$u(X_p) = \left| \frac{C_{X_2} - C_{X_1}}{X_2 - X_1} \right| \cdot \frac{X_{\max} - X_{\min}}{\sqrt{3}} \quad \text{Eq. 19}$$

In average the sensitivity coefficient was found to be 0.39 nmol/mol/V and assuming a voltage change of 20 Volts resulted in a standard uncertainty of $u(V)$ equal to 4.4 nmol/mol. One may observe that the effect occurred mainly at 210 V while between 220 and 230 V the sensor responses remained rather constant within 1 nmol/mol change that is consistent with the repeatability figure. In fact, applying a t test (unequal sample sizes 120 and 240 and unequal variances 8.8 and 7.7) between the average sensor response at 210 V and 220-230 V gave a t value of 3.06 showing that the difference is significant between these two groups of voltages.

7.7 Choice of tested interfering parameters in full factorial design

Even though the sensor was designed to measure both NO₂ and O₃, when the measurement of the sole O₃ is intended NO₂ acts as an interfering compound. The major cross sensitivities showed by the CairClipO3/NO₂ were in order of magnitude: NO₂, wind velocity, temperature, power supply, hysteresis of O₃ and humidity (see Table 22). Only the parameters whose standard uncertainty was higher than the short term drift were considered. NO₂, temperature and humidity which were found significant for the CairClipO3/NO₂ and the majority of the other sensors tested within MACPoll, were included in the experimental design even though the Cairclip compensation system for humidity was found effective.

Among the remaining factors:

- the estimation of the effect of wind velocity was not clearly established since the sensor did not work properly during this experiment. Moreover, it is unlikely that during field measurement, wind velocity would be measured and latter corrected. Consequently, wind velocity can only be estimated and taken into account when estimating the measurement uncertainty of the sensor results.
- the effect of power supply was found to be significant at low voltage. We consider that this effect can be avoided by assuring that that power supply remains within 220-230 V during field use.

Table 22: Summary of effect of all tested parameters

Parameters	Can be controlled?	Can be corrected?	$\Delta C/(\Delta X)$ (μ or n) mol/mol/Xunit	Standard uncertainty at LV
Laboratory calibration, nmol/mol		No	-	2.1
Repeatability, hourly values in a row		Not needed	-	0.6
Short term drift, after 1 day	No	Not needed	-	1.4
Long term drift, per days	No	Not needed	0.017	1.7
NO ₂ , nmol/mol	NO ₂ could be filtered for?	NO ₂ sensor needed	0.840	19.5 (for highest NO ₂ of 40 nmol/mol)*
NO, nmol/mol	Not needed	Not needed	0.005	0.1
CO, μ mol/mol	Not needed	Not needed	0.037	0.1
CO ₂ , μ mol/mol	Not needed	Not needed	0.000	0.0
NH ₃ , nmol/mol	Not needed	Not needed	0.010	1.0
SO ₂ , (not tested)				
Matrix effect	Unknown factors	Unknown, likely by field calibration?		1.1
Hysteresis of O ₃	No	It can be modelled?		0.7
Relative Humidity in %	Main effect is already controlled, slight hysteresis	The hysteresis effect might be corrected, sensor needed	0.008	1.4 (uncorrected)
Temperature, °C	?	Yes: but a T sensor is needed	0.24	4.6 or 1.9 if corrected
Wind, m/s	The sensor is already regulated for wind velocity. Protective box available	No: wind velocity sensor too expensive	-2.6	7.5**
Pressure, hpa	Not needed	Not needed	0.0411	1.2
Power supply, Volt	Voltage could be regulated between 220 to 230 Volt	No	0.390	4.4

* Correlation between NO₂ and O₃

** The estimation of the wind effect is suspicious since covariates were not independent during test and because of huge extrapolation

8 Experimental design

A factorial design of experiments was set up including the six O₃ levels of the pre-calibration experiment, 3 temperatures (12, 22 and 32 °C) under 3 relative humidities (40, 60 and 80%) and at 2 levels of NO₂ (0 and 95 nmol/mol). Table 24 shows the full factorial design of experiments with sensor responses. For the trial where several repetitions of tests were carried out, the sensor responses were averaged. In order to save time, the order of experiments was randomized for O₃ while they were not for temperature and humidity. Unfortunately, the Cairclip sensors were received after the test with NO₂ at 0 nmol/mol and temperature at 12°C and 32 °C were performed resulting in a loss of homogeneity of the experimental design. Moreover the test with O₃ at level at 20 nmol/mol had to be dropped because of the curvature of the pre-calibration curve at this test level. In this experiment, Eq. 2 could not be used because this model cannot compute O₃ at responses higher than at 179.0 (see Eq. 2) which was reached when O₃ and NO₂ were at their highest values. Consequently, the parabolic model (see Figure 6 at right) was used.

The dataset of measurement of the experimental design included the sensor responses and reference values for O₃, temperature, relative humidity, NO₂, NO, CO, ambient pressure, wind velocity and absolute humidity. As shows Figure 17, significant collinearities were observed between NO₂ and NO (same source of NO₂ but fortunately NO was shown not to be an interfering compound), between temperature/relative and absolute humidity (because H₂O was calculated using the Clausius-Clapeyron equation, see [4]) and between wind velocity and H₂O/temperature/relative humidity (this explains the effect of wind velocity on the sensor which is likely an effect of temperature in 7.4.2). It was chosen to design an experiment with

orthogonal factors: NO_2 , temperature, relative humidity and O_3 , they do not present any correlations. The biggest correlation between NO_2 and pressure was not important since pressure was found not to influence the sensor. Multi linear regression was used to model the sensor responses according to the available covariates within our dataset.

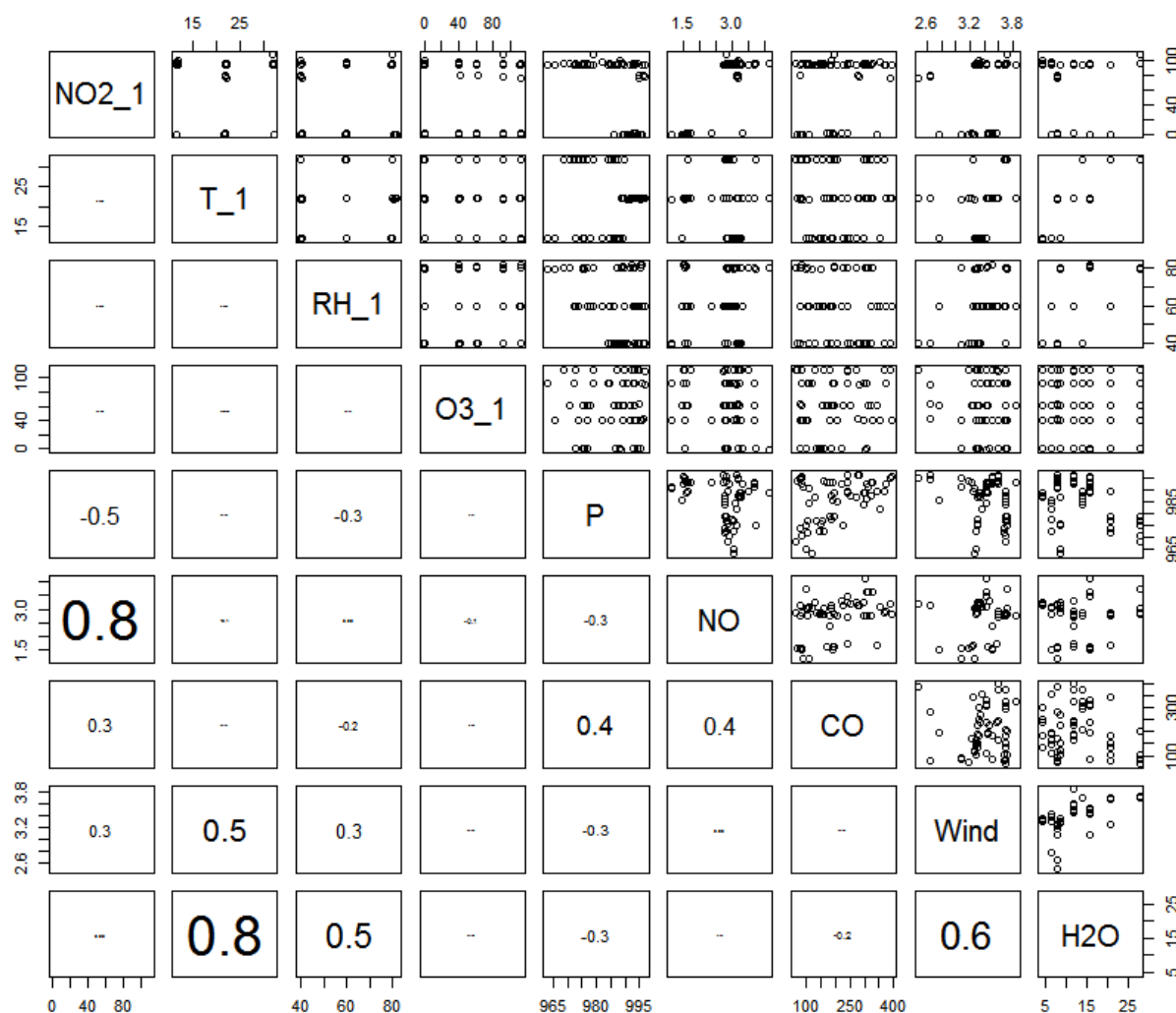


Figure 17: Collinearities of covariates (plots and coefficient of correlations) within the dataset of the experimental design for O_3 "O3_1", temperature "T_1", relative humidity "RH_1", NO_2 and NO in nmol/mol, CO $\mu\text{mol/mol}$, ambient pressure "P" in hPa, "Wind" velocity in m/s and absolute humidity "H2O" in mg/m³

Initially, all main effects were included in the Multi Linear Regression (MLR). Only NO_2 and O_3 were found significant. Therefore, temperature and humidity were dropped. Using the absolute humidity instead of the relative humidity led to the same conclusion: humidity did not affect the sensor responses. This is consistent with the results found in the single interference testing (see 7.4.1). When NO_2 was tested, a curvature of the sensor responses could be observed in the results. Therefore, the MLR was performed including NO_2 , O_3 and the square of these covariates. In this case, NO_2 , O_3 and the square of O_3 were found highly significant with a strong improvement of the residual standard error. Among the 2nd degree interactions, the one between NO_2 and O_3^2 was significant as expected. Keeping in mind that temperature was found to be a significant factor (see 7.4), we tried again to include temperature with NO_2 , O_3 , O_3^2 and NO_2 . O_3^2 -Temperature was then found significant.

The equation giving the sensor responses according to O_3 , NO_2 and temperature is given in Eq. 20 with Rs being pre-calibrated sensor responses (using the parabolic model, see 6.2), O_3 the reference UV-photometry ozone levels, T the temperature and NO_2 the concentration of nitrogen dioxide. Table 23 gives the multiple

analysis of variance which shows that all the effects and the interaction were highly significant (probability that these factors are not significant is < 0.04 %). It was checked that the residuals of the model equation were independent of all available covariates: reference values of O_3 , temperature, relative humidity, NO_2 , NO, CO, ambient pressure and wind velocity (see Figure 18)

$$R_s = -6.9 + 0.836 O_3 + 1.55 \cdot 10^{-3} O_3^2 - 6.43 \cdot 10^{-5} NO_2 O_3^2 + 1.07 NO_2 + 0.300 T$$

corresponding to

$$R_s = (1.55 \cdot 10^{-3} - 6.43 \cdot 10^{-5} NO_2) \cdot O_3^2 + 0.836 O_3 - 6.9 + 1.07 NO_2 + 0.300 T$$

Eq. 20

Table 23: Analysis of variance of the model equation

	Estimate	Standard Error	t-value	Probability (Pr(> t))
Intercept	-6.86	2.3110000	-3.0	0.0044
NO2	1.074	0.0183200	58.6	< 2 10 ⁻¹⁶
O3	0.836	0.0439400	19.0	< 2 10 ⁻¹⁶
O3 ²	0.001551	0.0004122	3.8	0.000404
Temperature	0.300	0.0692400	4.3	0.0000616
NO2 . O3 ²	-0.0000643	0.0000027	-23.8	< 2.10 ⁻¹⁶

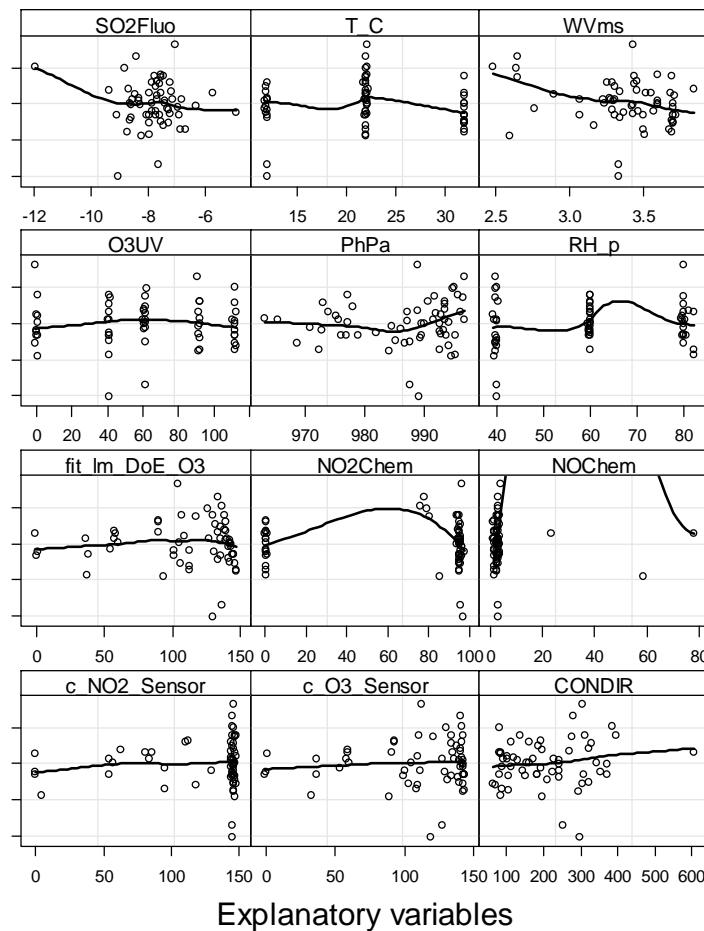


Figure 18: Relationships between residuals of the model equation and all available covariates including both the controlled and uncontrolled parameters

Table 24: Results of the design of experiments, the sensor results are calibrated with the parabolic model

NO2 nmol/mol	T °C	RH %	O3 nmol/mol	P hPa	NO nmol/mol	CO nmol/mol	Wind m/s	Sensor nmol/mol
0.7	11.9	60.0	61.1	986.0	1.6	345.3	3.2	55.1
0.4	22.0	40.0	0.3	994.2	1.6	77.8	3.2	0.5
0.4	22.0	40.1	40.9	996.6	1.6	90.9	3.2	36.9
0.5	22.1	40.1	61.2	993.4	1.6	173.0	3.2	60.0
0.4	22.0	40.4	91.8	995.8	1.6	113.5	3.2	93.3
0.4	22.1	40.1	112.4	994.1	1.5	70.1	3.2	109.3
0.8	22.1	59.9	0.4	992.8	2.2	NA	3.7	-0.5
1.1	22.1	60.0	41.0	991.9	1.7	208.4	3.7	36.4
0.9	22.2	60.0	61.2	991.3	1.8	NA	3.7	61.3
0.7	22.1	60.0	91.8	994.1	1.8	NA	3.5	93.7
1.3	22.1	60.0	112.2	992.6	1.7	270.5	3.8	110.9
0.4	21.8	80.0	0.5	995.1	1.6	82.2	3.2	-1.4
0.4	21.9	80.0	41.1	995.1	1.5	84.5	3.2	31.9
0.6	22.0	79.3	61.2	989.0	1.6	195.5	3.2	61.0
0.4	21.9	80.0	92.0	996.0	1.5	85.1	3.2	91.8
0.4	21.8	80.0	112.4	992.5	1.5	87.8	3.1	108.3
0.7	32.1	60.0	61.1	987.2	1.6	342.0	3.5	62.2
97.9	11.9	39.9	1.0	988.2	3.1	189.2	3.3	92.5
96.9	12.0	40.2	40.8	989.1	3.3	298.1	3.3	117.9
96.1	12.0	40.1	61.1	987.6	3.2	251.0	3.3	126.0
96.1	12.0	40.1	91.7	989.3	3.2	240.9	3.3	136.3
95.5	11.7	40.0	112.1	987.1	3.2	131.8	3.3	136.7
95.6	12.0	60.0	0.3	972.8	2.8	144.9	3.3	100.3
98.0	11.8	60.0	40.7	982.0	3.1	354.2	3.4	127.1
94.9	11.9	60.0	61.1	978.0	3.0	187.2	3.3	135.0
96.5	11.9	60.0	91.7	984.6	3.1	112.1	3.4	137.9
94.9	12.0	60.0	112.1	972.9	3.0	163.3	3.3	138.9
95.1	12.0	79.5	1.0	976.1	2.9	149.9	3.3	99.7
94.8	12.0	79.6	40.8	965.4	3.1	101.9	3.3	125.9
95.5	12.0	80.1	60.2	975.6	3.1	227.7	3.3	133.7
94.8	12.0	79.2	91.7	963.1	3.0	120.9	3.3	138.1
95.0	11.9	80.0	112.1	987.1	3.3	271.7	3.3	137.8
83.9	22.1	40.0	0.8	994.9	3.6	198.3	2.6	89.7
80.8	22.0	39.9	41.7	996.5	3.1	278.4	2.6	119.5
79.5	22.0	39.8	62.3	994.8	3.2	79.8	2.6	128.6
78.1	22.1	39.9	90.7	996.7	3.1	281.5	2.6	137.3
76.3	22.1	40.0	112.0	995.0	3.2	386.9	2.5	138.5
96.3	22.1	60.0	1.4	993.3	2.9	212.9	3.6	104.9
94.1	22.2	60.0	40.8	995.6	2.8	394.8	3.6	131.4
94.6	22.3	60.0	60.6	993.5	2.7	323.9	3.8	137.3
93.8	22.1	60.0	91.7	992.5	2.9	371.2	3.6	139.7
94.6	22.1	60.0	110.4	996.8	2.7	242.5	3.6	139.7

NO ₂ nmol/mol	T °C	RH %	O ₃ nmol/mol	P hPa	NO nmol/mol	CO nmol/mol	Wind m/s	Sensor nmol/mol
96.4	22.2	79.9	-0.6	988.8	4.1	304.4	3.4	111.9
95.8	22.1	80.0	40.7	993.4	3.7	329.8	3.4	131.8
94.4	22.0	80.0	61.1	991.7	3.6	311.0	3.4	138.9
96.1	22.1	80.0	91.7	992.9	3.7	309.8	3.4	139.6
94.9	22.1	80.0	112.1	989.9	3.5	240.8	3.4	139.0
95.1	32.0	39.9	-0.4	986.7	2.8	305.4	3.7	103.3
95.0	32.0	40.0	40.8	985.1	2.8	209.3	3.7	129.3
95.0	32.0	39.9	61.1	987.7	2.8	322.0	3.7	136.4
95.0	32.0	39.9	91.7	984.2	2.8	295.4	3.7	139.7
94.9	32.0	40.0	112.0	989.5	2.8	370.3	3.7	140.5
95.0	32.0	60.0	0.5	977.1	2.9	136.6	3.7	110.1
95.0	32.0	60.0	40.7	973.9	2.7	80.0	3.7	132.8
95.0	32.1	60.0	61.2	977.2	2.8	155.4	3.7	138.9
95.0	32.0	60.0	91.7	972.5	2.8	105.2	3.7	139.9
95.0	32.0	60.0	112.1	979.0	2.8	183.6	3.7	140.6
96.1	32.0	79.7	1.0	975.2	3.7	101.0	3.7	109.0
96.5	32.1	80.0	40.7	977.0	3.1	104.3	3.7	131.2
96.2	32.0	80.0	61.1	970.8	2.9	86.6	3.7	139.2
109.3	32.0	80.0	91.9	978.9	2.8	199.3	3.7	141.5
95.9	32.0	80.0	112.1	968.6	2.9	64.2	3.7	139.7

8.1 Uncertainty estimation

Finally, Eq. 20 can be solved to be able to estimate O₃, as given in Eq. 22. Obviously, the drawback of this equation is that it uses temperature and more problematic NO₂ as well.

$$O_3 = \frac{-0.836 + [0.836^2 - 4(1.55 \cdot 10^{-3} - 6.43 \cdot 10^{-5} NO_2)(1.07 NO_2 + 0.300 T - 6.9 - Rs)]^{1/2}}{2(1.555 \cdot 10^{-3} - 6.43 \cdot 10^{-5} NO_2)} \quad \text{Eq. 21}$$

$$u_c^2(O_3) = \sum \left(\frac{\partial O_3}{\partial x_i} \right)^2 u^2(X_i) \text{ and } U = k \cdot u_c \text{ with } k = 2 \quad \text{Eq. 22}$$

Which such a complicated model including 9 variables plus a second order polynomial, it would be too complicated to estimate the measurement uncertainty using the GUM method (see Eq. 22). Alternatively, we assume that the variance of the measurement is the sum of the variance of individual random variables including the contributions of the lack of fit of the model equation, NO₂ interference, temperature and humidity effect, hysteresis and matrix effect given in Table 25. The following observations apply:

1. The variance of the lack of fit of the model equation was estimated using the residuals of the laboratory model equation (Eq. 20). This parameter already includes contribution from the lack of fit of the calibration, the repeatability of sensor responses, and the short term drift: Hence these parameters are not repeated in the table.
2. In the column where the model equation is applied, the NO₂ contribution becomes null since it is corrected for. However, this implied that NO₂ has to be measured. Consequently an uncertainty for NO₂ measurements shall be considered. The NO₂ standard uncertainty was set by difference between the DQO and the rest of the parameter contributions resulting in standard uncertainty of 7.9 nmol/mol (expanded uncertainty U = 15.8 nmol/mol). Conversely, if the sensor values are not

corrected for NO₂ with the model equation then the NO₂ interference, u_{int} , found in Table 11 (19.5 nmol/mol) was taken into account.

3. As for NO₂, temperature was included in the model equation. In this case a measurement uncertainty of a temperature sensor shall be taken into account. A combined uncertainty of 1°C of the sensor results in a standard uncertainty of 0.2 nmol/mol taking into account the temperature sensitivity of 0.24 nmol/mol/°C.
4. Hysteresis: from the estimation of hysteresis, the repeatability of measurement figure ($S_r = 0.5$ nmol/mol) is subtracted which is already included in the lack of fit.
5. It was shown in 7.4.2 that relative humidity only affects the sensor by a kind of hysteresis effect to which the repeatability shall be subtracted rather than a systematic effect with a sensitivity coefficient.
6. Wind: in the absence of robust results no uncertainty contribution for the wind effect is taken into consideration
7. Power supply: according to the test in 7.6, we assume in the column with correction that power supply is controlled (between 220 and 230 V) allowing to avoid any effect of the power supply on the sensor responses. In the column at right without any correction or adjustment, the full effect estimated in 7.6 is taken into account after subtracting the repeatability of measurements.
8. Only in the case of correction of the sensor responses with the model equation the DQO was met. The main uncertainty contribution comes from the NO₂ effect.
9. As shown by experiments (see 7), no uncertainty contribution arose from drift of the sensor, hysteresis, pressure, CO, SO₂ and NO.

Table 25: Uncertainty after laboratory uncertainty at the O₃ limit value (60 nmol/mol)

	Parameters	Model applied + corrections/adjustments		Model not applied without corrections and adjustments
		correction?	Variance ^{1/2}	Variance ^{1/2}
1	Rs, lack of fit of model	yes	4.0	
2	NO ₂	yes	7.9*	19.5
3	Temperature	yes	0.2	4.6
4	Relative Humidity in %	no	(1.5 ² - 0.5 ²)	(1.5 ² - 0.5 ²)
5	Matrix effect	no	(1.1 ² - 0.5 ²) ^{1/2}	(1.1 ² - 0.5 ²) ^{1/2}
6	Hysteresis of O ₃	no	(0.7 ² - 0.5 ²) ^{1/2}	(0.7 ² - 0.5 ²) ^{1/2}
7	Wind, m/s	no	?	?
8	Power supply, Volt	Voltage adjusted 220-230 V	0	(4.4 ² - 0.5 ²) ^{1/2}
	U = 2 · u _c (see Eq. 22)		U = 2 × 9 nmol/mol ~ (DQO = 18 nmol/mol)	U = 2 × 20.6 > DQO ~ 70 %

*: obtained by difference between the DQO and the other contributions

9 Field experiments

9.1 Monitoring stations

The JRC station for atmospheric research and ambient air monitoring (45°48.881'N, 8°38.165'E, 209 m a sl) is located by the Northern fence of the JRC-Ispra site (Fig. 1), situated in a semi-rural area at the NW edge of the Po valley. The station is several tens of km away from large emission sources like intense road traffic or big factories. The main cities around are Varese, 20 km east, Novara, 40 km south, Gallarate - Busto Arsizio, about 20 km south-east and the Milan conurbation, 60 km to the south-east. Busy roads and highways link these urban areas. Four industrial large source points (CO emissions > 1000 tons / yr) are located between 20 and 50 km E to SE of Ispra. The closest (20 km SSE) emits also > 2000 tons of NO_x per year. The aim of the JRC-Ispra station is to monitor the concentration of pollutants in the gas phase, the particulate phase and precipitations, as well as aerosol optical parameters, which can be used for assessing

the impact of European policies on air pollution and climate change. Measurements are performed in the framework of international monitoring programs like the Co-operative program for monitoring and evaluation of the long range transmission of air pollutants in Europe (EMEP) of the UN-ECE Convention on Long-Range Transboundary Air Pollution (CLRTAP) and the Global Atmosphere Watch (GAW) Program of the World Meteorological Organization (WMO).

From May 2012 until October 2012, a mobile laboratory was installed near the EMEP station sited at Ispra, equipped with routine analysers normally installed in the containers. Gases were sampled using a sampling line (see Figure 19) placed at the top of the roof of the van at about 3.5 m above the ground and on the roof of the mobile laboratory. The sampling line consists in a stainless steel gas inlet with grid protection for rain, insects and dust. The stainless steel inlet tube of 4 cm internal diameter with internal PTFE tube that ends with a Teflon manifold of 8 PTFE ports to connect the gas analysers. The sampling line is flushed with ambient air with about 2 second resident time of samples. Each instrument samples from the glass tube with its own pump through a ¼" PTFE/PFE tube and a 1 µm pore size 47 mm diameter Teflon filter to eliminate particles from the sampled air.

The mobile laboratory was equipped with meteorological sensors and gas analysers which were calibrated in laboratory before the in-situ measurements and then checked every month. Field checks were carried out using zero air in gas cylinders and a span value (internally certified gas cylinders at low concentration for NO/NO_x and SO₂, highly concentrated cylinders for CO and ozone generator do O₃). The highest observed drift of calibration was 3 %, consistent with the uncertainty of the working standards used on field. Therefore, no correction of measurements was undergone apart from the discarding values during maintenance and calibration checks.

- Meteorological parameters (ambient temperature, ambient relative humidity, ambient pressure, 10m mast for wind speed and wind direction) a mobile. The mobile laboratory was equipped with:
- Gaseous pollutants: for O₃ an UV Photometric Analyzer Thermo Environment 49C; for NO₂/NO/NO_x a Chemiluminescence Nitrogen Oxides Analyzer Thermo 42C; for CO a non-Dispersive Infrared Gas-Filter Correlation Spectroscopy Thermo 48C-TL, for SO₂ and UV Fluorescent Analyser Thermo 43C TL

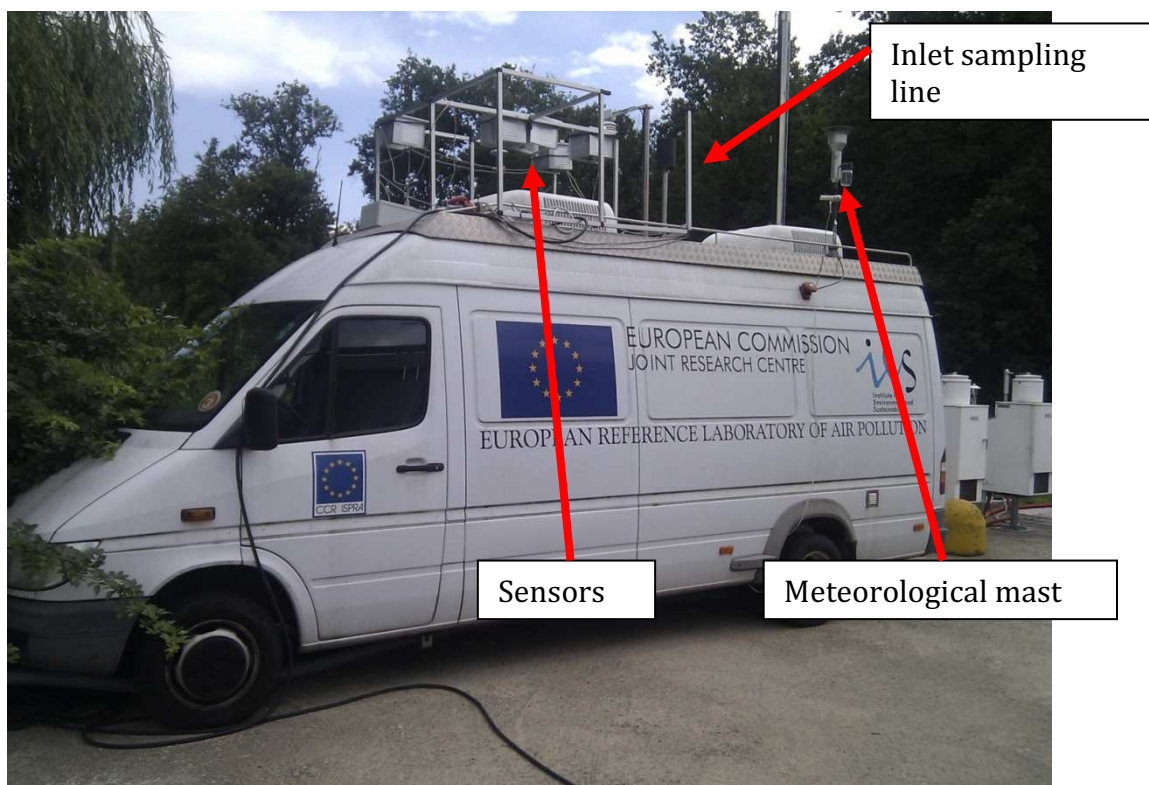


Figure 19: mobile laboratory used that the EMEP station of JRC Ispra.

9.2 Sensor equipment

To avoid interference, we made sure that the flow air coming out of the air condition system was blowing far enough from the sensor to avoid any effect on the sensor responses.

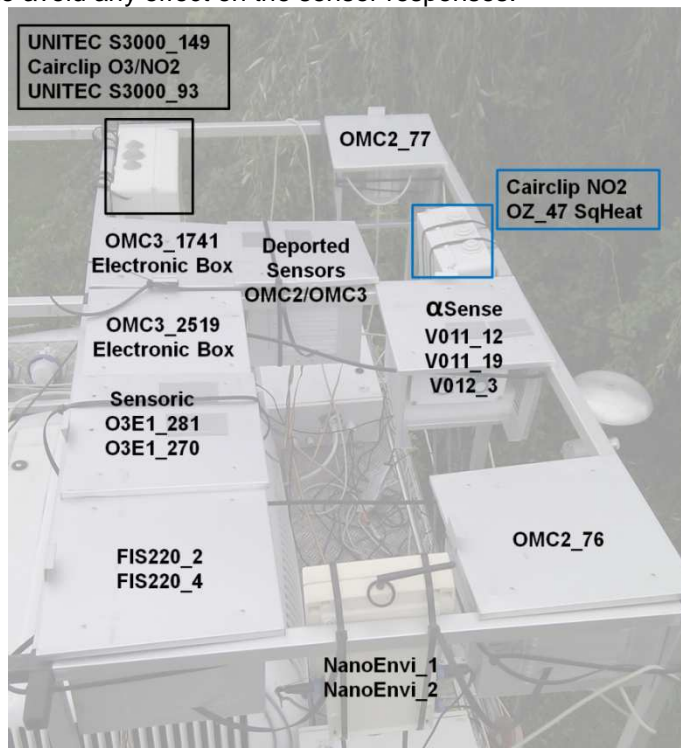


Figure 20 Sensors location at the monitoring station

9.3 Check of the sensor in laboratory

Hopefully, the sensor should have been tested in laboratory before installation in field. However, the exposure chamber was busy with the laboratory tests when receiving the field sensor and the laboratory check had to be postponed to the end of the field experiment. Consequently, the field sensor was submitted to a lab tests at the end of the field experiment as described in 7.3. During experiment, NO₂, temperature and humidity were kept under control. The temperature and relative conditions of the test were set at 22°C and 60 % of relative humidity, the defined mean values.

The results of the experiment are given in Figure 1 which shows that little or no curvature of the field sensor responses, conversely to what was observed for the lab sensor (6.2). A simple linear equation was sufficient for this sensor. Consequently, it was expected that the field sensor would give a linear response during the field experiment.

The pre-calibration functions were established by plotting sensor responses versus reference values measured by the TECO 49C analyser (see Figure 6) of relative humidity. Each steps lasted for 150 minutes once the condition of O₃ concentrations, temperature and humidity were reached. The averages of the last 60 minutes were plotted. For the field experiment, the calibration functions established in this tests was not systematically applied.

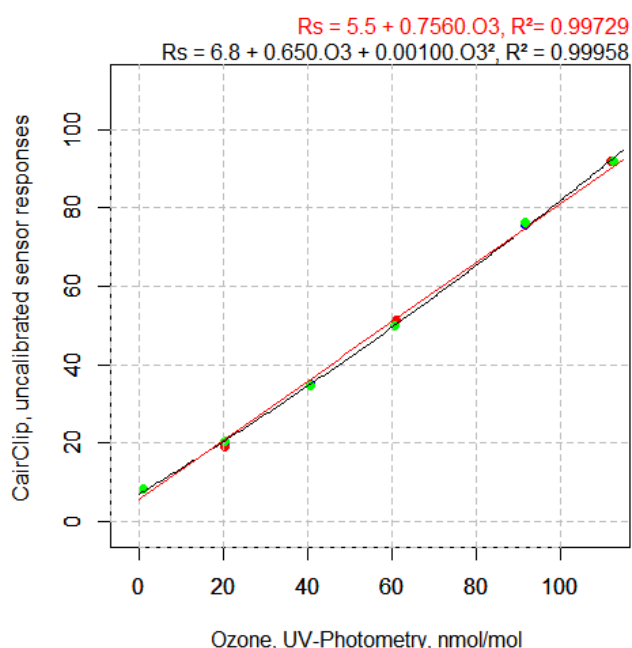


Figure 21: Initial calibration of Cairclip sensor used for the field experiments at 22

9.4 Field Results

The Cairclip sensors were installed in field between 25 June and 02 October 2012. However, due to some error of the data acquisition system, valid measurements started to be recorded from 19 July only. Apart from the sensor responses, reference values were registered for O₃, NO₂ and NO, SO₂, CO, PM₁₀, temperature, solar radiation, relative humidity while absolute humidity was calculated. However, the time series for PM₁₀ and solar radiation being incomplete they had to be dropped.

Abnormal high values for NO and CO at rural sites were seldom observed (6 hourly averages were discarded) even though they had no effect on the agreement between the sensors and the analysers values.

Being in field where factors cannot be controlled, collinearities between each other is unavoidable (see Figure 22). In particular, there were strong correlations between O₃, temperature and humidity as expected, making it impossible to include all of these parameters into a regression model. A lower level of correlation could be also observed between O₃ and wind (both in direction and velocity as they are auto correlated). Opportunely, the sensor responses were highly correlated with reference O₃ levels but it was also associated with temperature and humidity as a consequence of their natural correlation. It is more difficult to guess if the correlation between the sensor response and the wind was coming from its correlation with O₃ or from a effect between wind and the sensor responses. In fact, the variance inflation factor of O₃, NO₂, NO, SO₂, CO and absolute humidity were up to 2.0 showing acceptable level of collinearities between all of them.

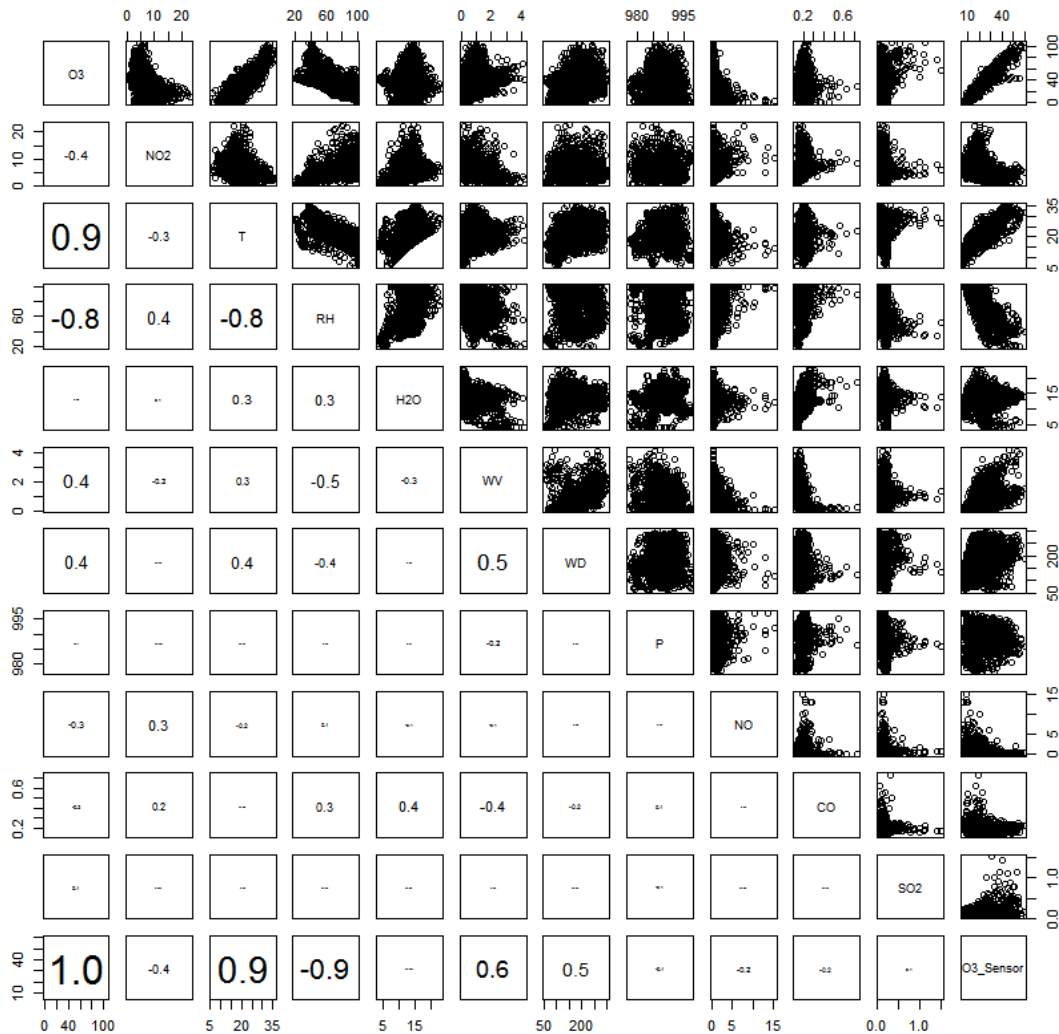


Figure 22: Collinearities in the field data set with scatterplots between pairs of parameters (upper matrix plots) and their correlation (lower matrix values) for hourly values of O_3 , NO_2 , NO , and SO_2 in nmol/mol, CO in $\mu\text{mol/mol}$, temperature in $^{\circ}\text{C}$ (T), relative humidity in % (RH), absolute humidity in mg/m^3 (H_2O), wind direction in $^{\circ}$ (WD), wind velocity in m/s (WV) and pressure in hPa (P). O_3 .

Subsequently different treatment was applied to the sensor responses which were plotted against the reference O_3 measured by UV photometry. Figure 23 shows in order of appearance:

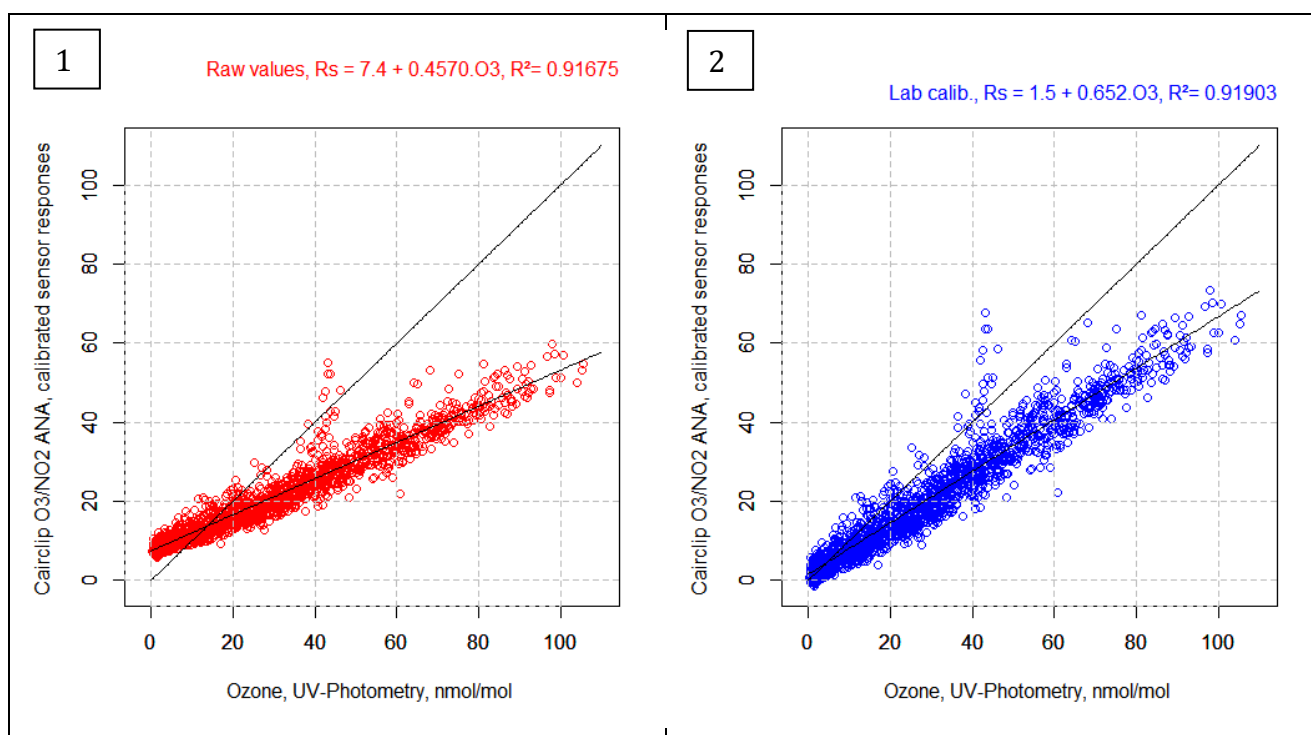
1. Raw sensor responses against reference O_3 : the response are highly linear with high coefficient of determination ($R^2 = 0.917$) but with a slope and interception of the regression line different from 1 and O , respectively. A few abnormal values appears towards 40 nmol/mol .
2. Sensor responses after calibration using the pre-calibration function established in laboratory (see 9.3), both the agreement between the sensor and UV-photometry improved with the slope increasing from 0.45 to 0.65, the intercept decreasing from 7.4 to 1.5 and a slight increase of the coefficient of determination. Nevertheless the slope being different from 1, this shows that laboratory calibration does not ensure full agreement between sensor responses and UV photometry in field.
3. Application of the laboratory model (Eq. 21) to the sensor response calibrated with the laboratory calibration function did not improve further the data: the slope only slightly improves (0.68 instead of 0.65) but the coefficient of determination slightly worsened (0.89 instead of 0.92). In fact the model was designed for both high levels of O_3 and NO_2 while only low levels of NO_2 were registered during the field campaign.

The manufacturer gave this information: because of the electrolyte, electrochemical sensors need a minimum humidity in the atmosphere. Low humidity can lead to a diminution of the electrolyte

volume and consequently to an increase of the signal which is proportional to its concentration in the electrolyte.

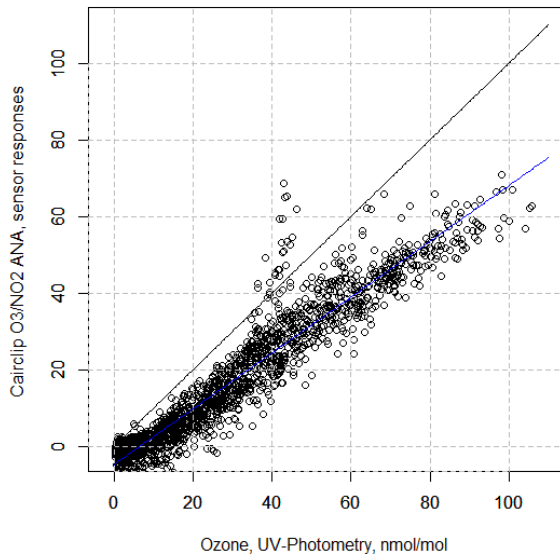
On the plots 1 to 3 of Figure 23, a few abnormal peak values appeared at about 40 nmol/mol of O_3 . Generally, they demonstrated homogeneity of variance between the residuals and the fitted variables (fit_lm_Field_O3) apart from the peak values at 40 nmol/mol. In order to investigate these values, a linear line was fitted between the sensor responses and the reference O_3 . The residuals of this linear model were plotted against all covariates (see Figure 24). It appeared that the high residuals values were associated with low values of humidity (relative and absolute), NO and NO_2 , SO_2 and CO and high wind velocities. The sole causality relation that we could find was that at low relative humidity, the cellulose buffer used for adjusting the relative humidity of the sensor may not be effective and hence disturbing the sensor correct operation. It was thus decided to discard the sensor values when relative humidity was < 35 %.

4. Calibration of the sensor responses versus reference O_3 during the 1st week of measurements.
5. Sensor responses from the 2nd week of the measuring campaign versus reference O_3 with relative humidity < 35 % discarded. The sensor is calibrated on field during the 1st week of the field campaign by comparison to the UV-photometry analyser.
6. The same treatment as in plot 5 adding the application of the model equation (Eq. 21) established in the laboratory. A little improvement occurs that maybe not worth since temperature and NO_2 were needed. It is possible that in situation where high NO_2 and O_3 are registered, the model equation would have been more effective.



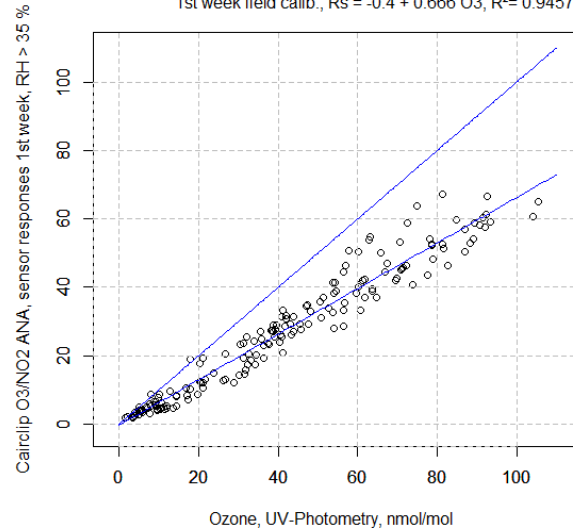
3

Lab calibration + Lab. model, $R_s = -4.8 + 0.728 O_3$, $R^2 = 0.90131$



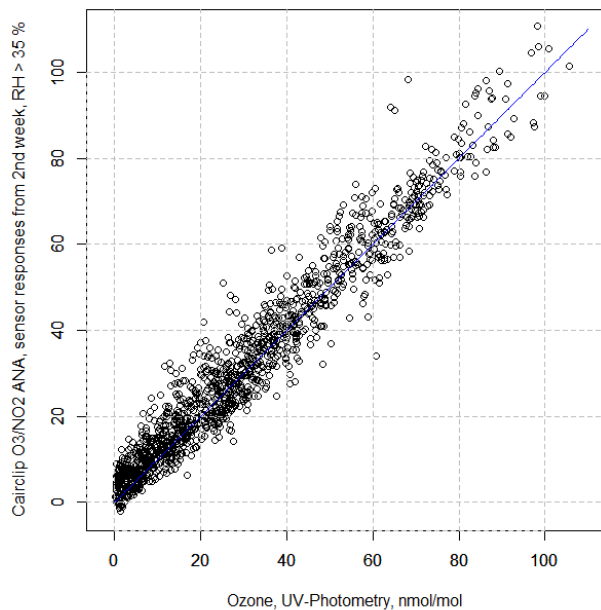
4

1st week field calib., $R_s = -0.4 + 0.666 O_3$, $R^2 = 0.9457$



5

Lab calib., 1st week field calib., $R_s = 2.8 + 0.972 O_3$, $R^2 = 0.9419$



6

Lab calib., 1st week field calib., Model Equation, $R_s = -2.7 + 1.044 O_3$, $R^2 = 0.9470$

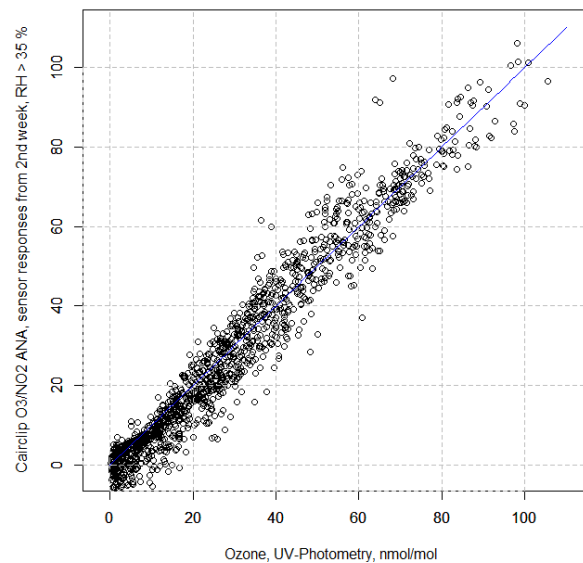


Figure 23: Sensor responses versus O_3 reference values. Upper left: raw sensor responses; upper right: laboratory calibrated sensor responses; middle left: laboratory calibrated sensor responses and application of the laboratory model equation; middle right: calibration during the 1st week of measurement; Bottom left: sensor responses from the 2nd week of the campaign, field calibrated with data of the 1st week, without values with relative humidity < 35 %; Bottom right the same as bottom left with application of the laboratory model equation.

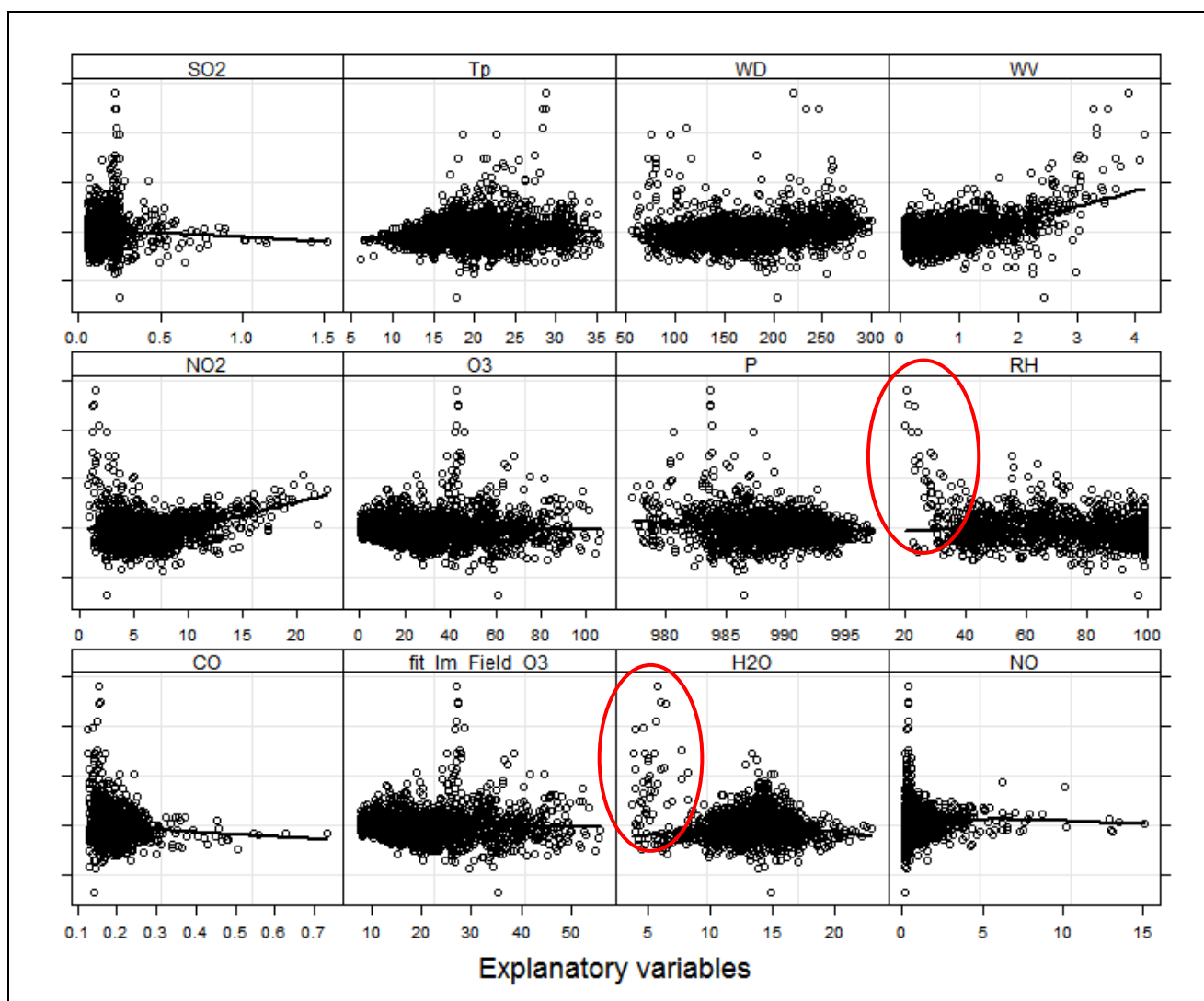


Figure 24: Relationship between the residual of the linear model between the sensor response and O_3 measured by UB and all available covariates. “fit_lm_field- O_3 ” represents the sensor fitted values of the linear model. In red circle the abnormal values with high residuals.

9.5 Estimation of Field uncertainty

The field uncertainty was calculated by comparing the sensor results with the reference O_3 using the methodology described in the guide for the demonstration of equivalence [7], and given in Eq. 23 to 25. Eq. 23 gives the underlying linear model between reference measurements (x) consisting of the UV-photometry measurements and sensors values (Y). Eq. 24 gives the uncertainty of the sensor values where RSS is the sum of the relative residuals resulting from the orthogonal regression of the sensor values versus reference O_3 according to Eq. 25. In Figure 23, the residuals appeared to be constant giving a justification to use Eq. 25. $u^2(x_i)$ the random uncertainty of the reference measurements was set to 1.5 nmol/mol according to the CEN standard[8]. The last term in Eq. 24 gives the bias of the gas sensor at the limit value/target value x_i . The algorithm to estimate a and b, the slope and intercept of the orthogonal regression together with their uncertainty is given in the Guide for the demonstration of equivalence [7].

$$Y_i = a + bx_i$$

Eq. 23

⁷ Guide to the demonstration of equivalence of ambient air monitoring methods, Report by an EC Working, Group on Guidance

⁸ EN 14625:2005 ‘Ambient air quality - Standard method for the measurement of the concentration of ozone by ultraviolet photometry’

$$u^2(Y_i) = \frac{RSS}{(n-2)} - u^2(x_i) + [a + (b-1) \cdot x_i]^2 \quad \text{Eq. 24}$$

$$RSS = \sum (y_i - b_0 - b_1 x_i)^2 \text{ if } (y_i - b_0 - b_1 x_i)^2 \text{ is constant} \quad \text{Eq. 25}$$

Sensor may be accepted as indicative method if the field uncertainty is lower than the laboratory uncertainty or if it does not exceed the DQO. Without field calibration (not this case), if a and b were not significantly different from 0 and 1, respectively, the laboratory model equation would be considered valid for any field situation of the same type (background/rural). Figure 25 shows the extent of the relative expanded uncertainty ($U_r = k \cdot u(Y_i)$ with $k = 2$) versus reference O_3 . Only the data registered after the 1st week of the campaign was considered to avoid concluding using the calibration data. Two data treatments were considered:

- the red line which gives the sensor responses calibrated during the 1st week after discarding relative humidities < 35 %.
- the blue line which gives a slight decrease of the measurement uncertainty by applying the laboratory model equation (Eq. 21) to the previous data.

In both cases the Data Quality Objective is met with relative expanded uncertainty of about 20 % lower than 30 % at the limit value.

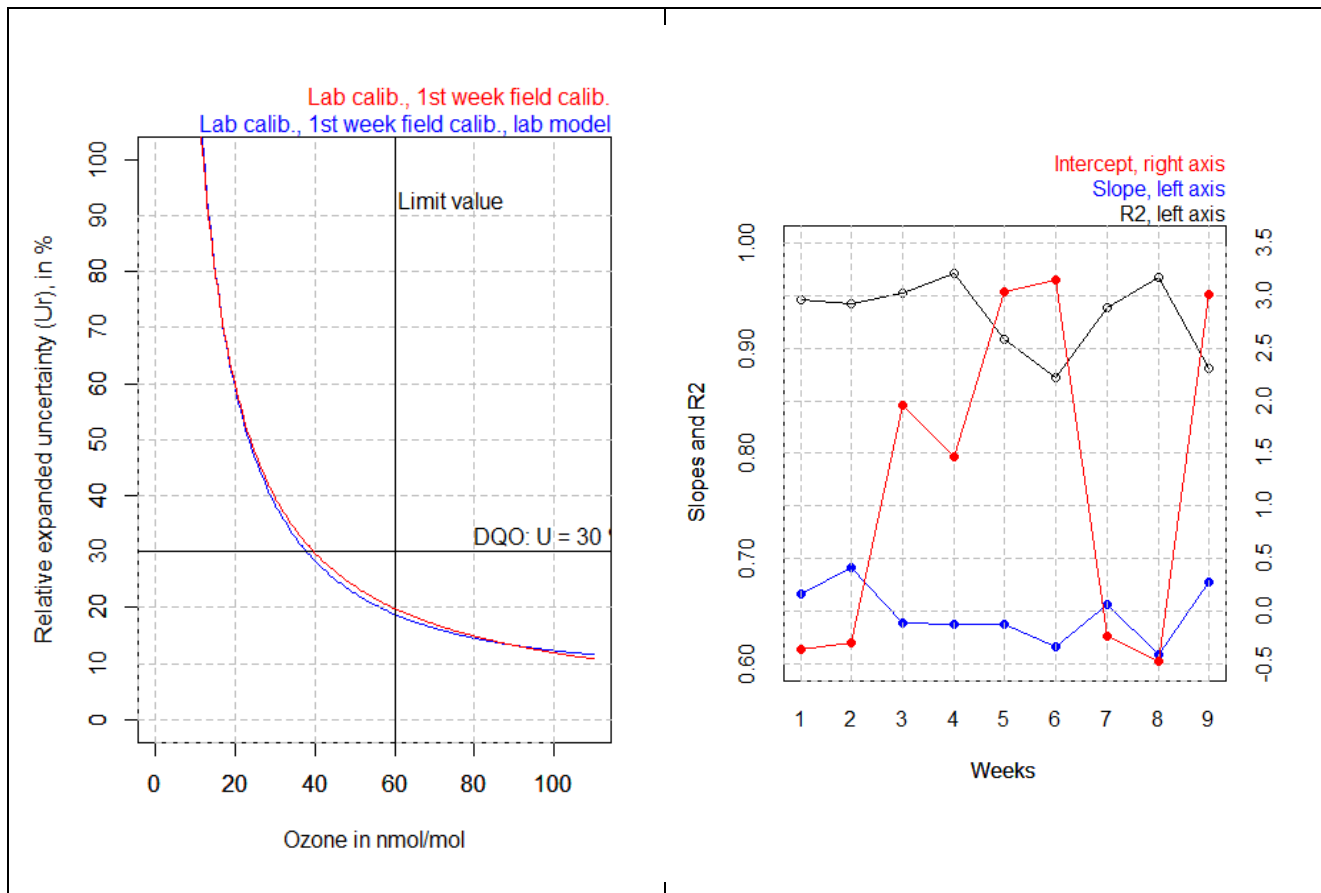


Figure 25: left: relative expanded uncertainty of the Cairclip sensor responses versus O_3 reference concentration. Right: weekly trend of field calibration (slope, intercept and coefficient of determination)

9.6 Calibration

This paragraph is based on the observations of the sensor used for the field experiment. The sensor used for the lab experiment did not give a linear response. The manufacturer reported that this was unusual (in their



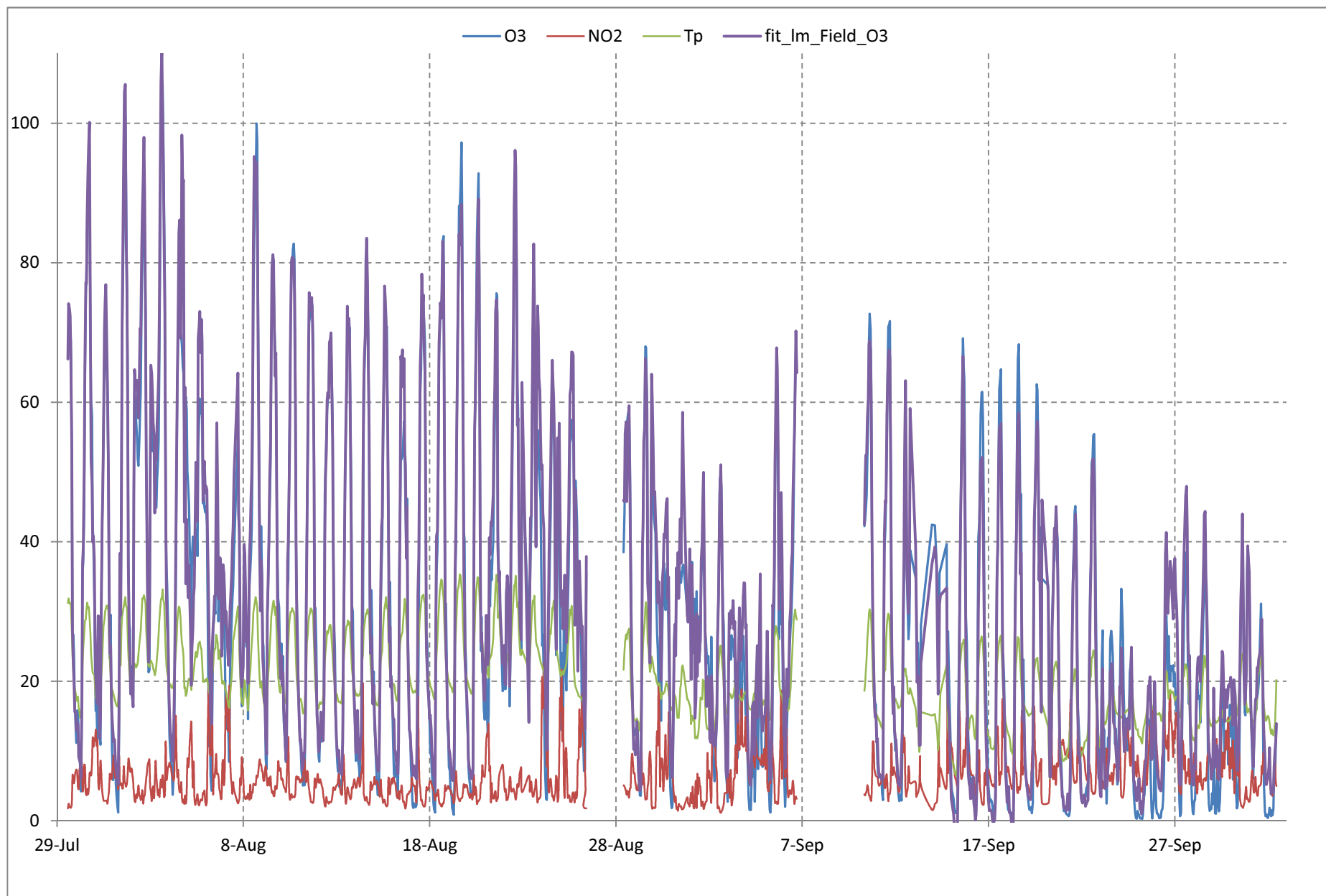
experience, the sensor is linear). Anyhow all conclusions drawn from the field sensor could be applied to any sensor provided that its response is made linear using for example a laboratory calibration.

The sensor used at the field site was not previously calibrated by the manufacturer at reception.

1. During the field experiment, the sensor was found linear. The calibration function was: $R_s = 7.4 + 0.457 O_3$ where O_3 was reference values measured by UV-photometry.
2. In laboratory, the sensor showed a linear relationship. However, the calibration function was different than the one observed in field: $R_s = 5.5 + 0.756 O_3$ (see 9.3). The manufacturer argued that this difference was the result of an exceptional conditioning problem. However, three replicated calibrations in the laboratory gave the same calibration function. The application of the laboratory model equation (Eq. 21) did not produce better agreement with UV-photometry in this case.
3. Conversely, it was observed that the sensor responses of 10 weeks of field measuring campaign could agree with UV-photometry provided that the sensor was calibrated during the 1st week of comparison sensor versus UV-photometry.
4. Once the sensor was calibrated during the 1st week, provided that this period included the whole range of O_3 conditions, the sensor was shown to keep on agreeing with UV-photometry for 10 weeks. The application of the laboratory model equation (Eq. 21) led to slight improvements while temperature and NO_2 were needed in the model equation. NO_2 was very low during the field experiment; it is possible that if it was higher the model equation would have been more effective.
5. Re-calibration was not found necessary during the whole field campaign since the calibration function did not show any trend both in the laboratory and field experiments. Some random noise in these data cannot be avoided because of the timely change of concentration levels. The re-calibration periodicity can be set to the whole duration of the field campaign: 1+9 weeks.

Our observation was that calibration of the sensor shall be carried out during field experiment by comparison to reference measurements. It is likely that the validity of this observation is limited to the monitoring site of the field experiment. .

The figure next page presents the trend of the sensor responses in nmol/mol calibrated during the 1st week without relative humidity lower than 35 %. The figure also shows reference O_3 in nmol/mol, temperature in °C and relative humidity in %.





10 Conclusions

The main advantages of CairclipO₃/NO₂ sensor compared to other sensor were that it did not suffer long term drift and that it was free from humidity effect. This was confirmed during the field experiment provided that relative humidity did not reach too low values (RH < 35 %).

The CairclipO₃/NO₂ is designed to measure both O₃ and NO₂. When monitoring the sole O₃, the major drawback of the sensor is its sensitivity to NO₂ that may prevent from correctly estimating O₃ if high levels of NO₂ and O₃ are simultaneously present in the sampled air. In this study it was decided to evaluate the sensor at sites where NO₂ and O₃ are not simultaneously at high levels namely background sites at rural areas.

In laboratory, a number of experiments showed that the sensor is in fact highly sensitive to NO₂ but is independent from change of CO, NO, CO₂ and NH₃. The sensor did not undergo short and long term drift, it was not sensitive to pressure changes and did not present hysteresis effect when ozone changes. It was slightly dependent to temperature and power supply changes that needs to be controlled. It showed little hysteresis when relative humidity changes. Some doubts remain about the sensitivity of the sensor to wind velocity.

A sophisticated model equation was established in laboratory that needs NO₂ and temperature to estimate O₃. In laboratory and at high NO₂ levels, when using this model the measurement uncertainty was found lower than the Data Quality Objective of the European Directive for measurement while the DQO would not be met without.

However, the effectiveness of the laboratory model equation was not easily demonstrated with the results of the field campaign for several reasons. Firstly, the calibration function of the field sensor was nearly linear while the one of the laboratory was clearly parabolic. The manufacturer suggested that this difference might be the result of different conditioning effect of the sensor during this study. Secondly, the laboratory model equation was designed to improve the sensor responses in case of high NO₂ levels. However, the measuring campaign took place at rural areas and in summer when O₃ levels are high with low NO₂ levels. In this case, the Cairclip sensor showed a linear response without applying the laboratory model equation which could not further improve the sensor agreement with the UV-photometry method. It would be interesting to estimate the efficiency of the model equation when NO₂ is higher.

Conversely to the manufacturer experience, our observation was that the Cairclip sensor could not only rely on the calibration carried out in laboratory model nor a simple adjustment. A field calibration of one week was found effective for a 10-week period of used. Both in laboratory and in field, it was found that re-calibration of the sensor was not necessary over a 10-week measuring campaign.

The Data Quality Objective of indicative method of the European Directive is met by the CairClipO₃/NO₂. In fact, at the limit value of 60 nmol/mol, the relative expanded uncertainty of the sensor measurements was found to be about 20 % while the DQO is 30 %. Applying the laboratory model equation only improved the relative expanded uncertainty to 19 %.

Since, the laboratory model equation resulted in a high bias when used in field measurement and that the sensor needed to be calibrated for field use, it is advised to confirm the sensor measurement by comparison to the UV-photometry method.

Further to this study, the field of application of the Cairclip sensor is validated for fixed measurement at background site/rural areas provided that the sensor is calibrated by comparison to the UV-photometry method before normal use.



11 Appendix A: Technical Data Sheet Cairclip O₃-NO₂



MINIATURE AIR QUALITY MONITORING SYSTEMS
P049D.OZ.Technical Data Sheet O₃-NO₂.160812

Technical Data Sheet CairClip O₃-NO₂

(document prone to modifications)

Range	0-250 ppb (0 - 240 ppb analog)
Limit of detection ^(1, 2)	20 ppb
Repeatability at zero ^(1, 2)	+/- 7 ppb
Repeatability at 40 % of range ^(1, 2)	+/- 15 %
Linearity ^(1, 2)	< 10%
Uncertainty	< 30% ^(2, 3)
Short term zero drift ^(1, 2, 4)	< 5 ppb/24 H
Short term span drift ^(1, 2, 4)	<1% FS ⁽⁵⁾ /24 H
Long term zero drift ^(1, 2, 4)	< 10 ppb/1 month
Long term span drift ^(1, 2, 4)	< 2% FS ⁽⁵⁾ /1 month
Rise time (T10-90) ^(1, 2)	<90s (180s if large variation of RH)
Fall time (T10-90) ^(1, 2)	<90s (180s if large variation of RH)
Effect of interfering species ⁽¹⁾	Cl ₂ : around 80% Reduced sulphur compounds : negative interference
Temperature effect on sensitivity ⁽²⁾	< 0.5 % / °C
Temperature effect on zero ⁽²⁾	+/- 50 ppb maximum under operating conditions
Maximum exposure	50 ppm
Annual exposure limit (1 hour average)	780 ppm
Operating conditions	- 20°C to 40°C / 10 to 90% RH non-condensing 1013 mbar +/- 200 mbar
Recommended storage conditions	Temperature: between 5°C and 20°C Air relative humidity: > 15% non-condensing
Power supply ⁽⁶⁾	5 VDC/200mA (rechargeable by USB via PC or 100V-240V/5V 0.8A-1.0A with adapter)
Communication interface	USB, UART Analog (UART & 4-20 mA / 0-5 V converter)
Dimensions	Diameter: 32 mm - Length: 62mm
Weight	55g
Protection	IP42 (according IEC60529)
Electrical certification	 Conform to UL Std. 61010-1 Certified to CSA Std. C22.2 N°. 61010-1 
Parameters Set up / Downloading	CairSoft

¹ According to our operating conditions during tests in laboratory: 20°C +/- 2°C / 50% RH +/- 10% / 1013 mbar +/- 5%.

² Values possibly affected by exposures to high gradients of concentration

³ In accordance with the Directive 2008/50/EC of the European Parliament and of the Council of 21 May 2008 on ambient air quality and cleaner air for Europe

⁴ Full scale continuous exposure

⁵ FS = Full Scale

⁶ The complete discharge of a device (screen turned off) can lead to a deterioration of its performances

Any use of the sensor not complying with the conditions specified in herein, including exposures, even short ones, to environments other than ambient air, to dry and / or devoid of oxygen air or other atmosphere not composed in majority of air, even during calibration, will invalidate the warranty.

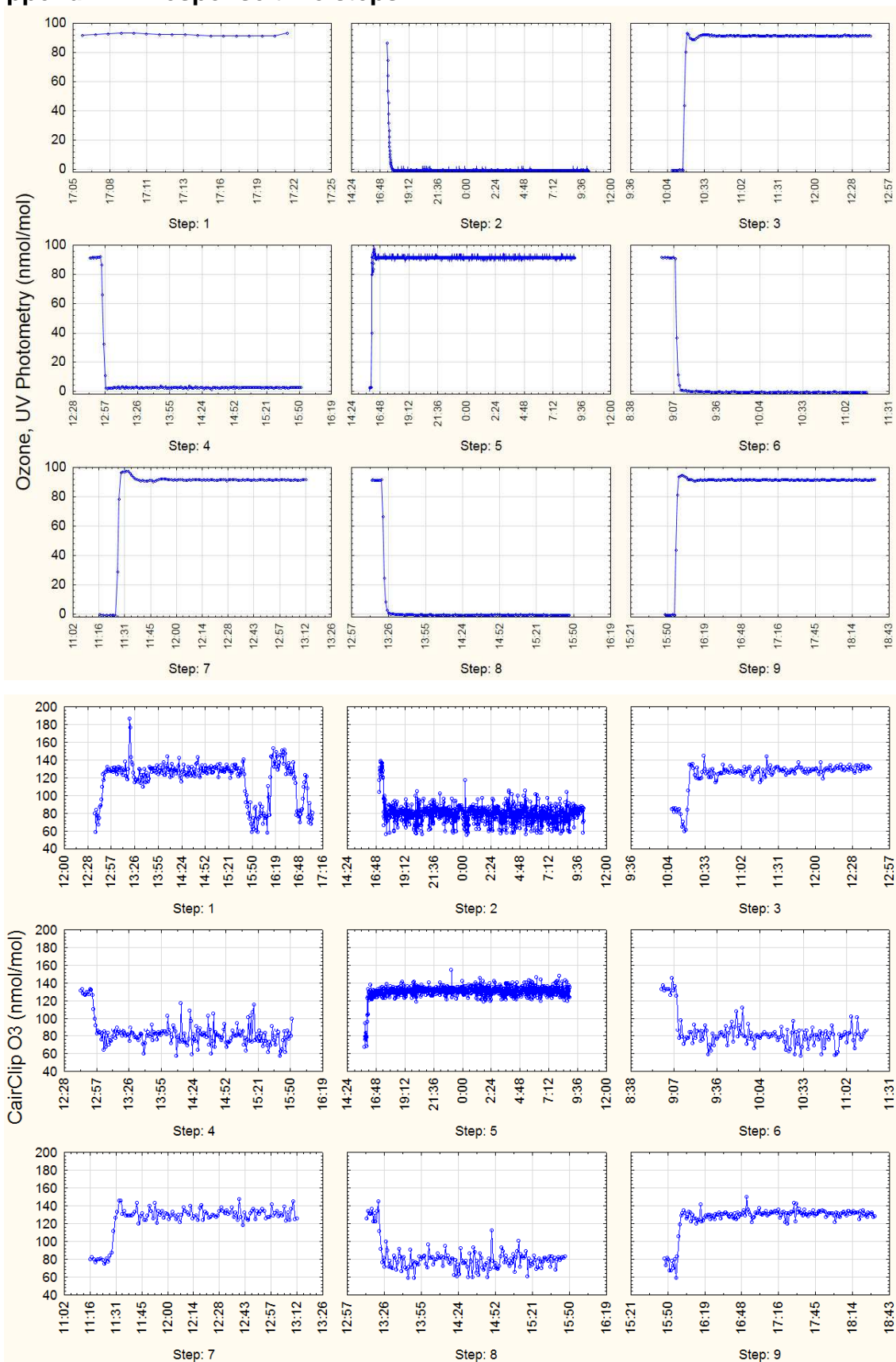
Main options	CairTub: autonomy 21 days CairNet: wireless communication & battery powered by solar panel Software: CairSoft, CairMap, CairWeb
---------------------	---

Office : CAIRPOL
ZAC du Capra
55, avenue Emile Antoine
30340 Méjannes les Alès - France

SARL au capital de 354 200€ - N° Siren : 492 976 253

Tel: +33 (0)4 66 83 37 56
Fax: +33 (0)4 66 61 82 53
info@cairpol.com
Web site: www.cairpol.com

12 Appendix B: Response time steps



European Commission

EUR 26373 – Joint Research Centre – Institute for Environment and Sustainability

Title: Report of laboratory and in-situ validation of micro-sensor for monitoring ambient air pollution

Author(s): Laurent Spinnelle, Michel Gerboles and Manuel Aleixandre

Luxembourg: Publications Office of the European Union

2013 – 59 pp. – 21.0 x 29.7 cm

EUR – Scientific and Technical Research series – ISSN 1831-9424 (online)

ISBN 978-92-79-34832-7 (pdf)

doi: 10.2788/4277

Abstract

The aim of this report is to evaluate and validate CairClipO3/NO2 sensors of CAIRPOL with laboratory and field tests under ambient/indoor air conditions corresponding to a specific micro-environment: background station, rural areas. This report presents the evaluation of the performances of the sensor and the determination of its laboratory and field measurement uncertainty compared to the Data Quality Objective (DQO) of the European Air Quality Directive for indicative method. Further, procedures for the calibration of sensors able to ensure full traceability of measurements of sensors to SI units are developed.

As the Commission's in-house science service, the Joint Research Centre's mission is to provide EU policies with independent, evidence-based scientific and technical support throughout the whole policy cycle.

Working in close cooperation with policy Directorates-General, the JRC addresses key societal challenges while stimulating innovation through developing new standards, methods and tools, and sharing and transferring its know-how to the Member States and international community.

Key policy areas include: environment and climate change; energy and transport; agriculture and food security; health and consumer protection; information society and digital agenda; safety and security including nuclear; all supported through a cross-cutting and multi-disciplinary approach.

